6-15-2020 1:30 PM

Investigating the Regulation of Fatty Acid Efflux Pump FarE by TetR Family Regulator FarR in Staphylococcus aureus

Katherine A. Ferguson, *The University of Western Ontario*

Supervisor: McGavin, Martin J., *The University of Western Ontario*

A thesis submitted in partial fulfillment of the requirements for the Master of Science degree in Microbiology and Immunology

Abstract

The success of the USA300 strain of methicillin resistant *Staphylococcus aureus* can be attributed in part to its enhanced ability to overcome innate defenses of the skin including sebum, which provides a source of antimicrobial unsaturated free fatty acids (uFFA). We have previously identified *farE* and *farR* genes that confer *S. aureus* resistance to uFFA, respectively encoding a uFFA efflux pump and a TetR family regulator required for *farE* expression. However, the exact regulatory mechanism of FarR remains to be elucidated. Here, we show the importance of a conserved TAGWTTA motif in FarR operator sites, such that the loss of this motif in autoregulatory operator sites caused a de-repression of FarR. However, this de-repression did not cause an increase in resistance to uFFA. Additionally, we have identified the importance of cysteine residues for FarR function. These findings shed further light on the mechanisms of *S. aureus* resistance to antimicrobial uFFA.

Keywords: Antimicrobial fatty acids, RND family efflux pump, TetR family regulator, *Staphylococcus aureus*, *farR*, *farE*

Summary for Lay Audience

Staphylococcus aureus colonizes approximately 30% of the population asymptomatically and yet can cause mild to severe infections. Frequently, these infections are caused by the colonizing strain. Therefore, understanding the mechanism by which *S. aureus* persists on, and colonizes the skin is of importance. USA300 is the predominant strain of community acquired methicillin resistant *S. aureus* in North America and is the leading cause of skin and soft tissue infections. The success of USA300 can be attributed in part to their enhanced ability to overcome the immune defences of the skin, which include fatty acids that are found in the sebum. These fatty acids are toxic and therefore, USA300 employs several strategies to overcome this toxicity. One way is through the removal of fatty acids from the bacterial cell through the protein FarE. Here, we further study the regulation of FarE by its regulator, FarR. Overall, these findings shed further light into fatty acid resistance strategies employed by *S. aureus*.

Co-Authorship Statement

Portions of this thesis have been published:

Alnaseri H., Kuiack R.C., Ferguson K.A., Schneider J.E.T., Heinrichs D.E., McGavin M.J. 2019. DNA binding and sensor specificity of FarR, a novel TetR family regulator required for induction of the fatty acid efful pump FarE in *Staphylococcus aureus. J bacteriol.* 201(3) e00602-18

Robert Kuiack performed the native *farER*^{IS} EMSA (Fig 3.1B).

Acknowledgements

I would first like to express my deepest gratitude to my supervisor Dr. Martin McGavin as this project would not have been possible without his support and guidance. Thank you for taking a chance on me as an undergraduate student, it was an invaluable learning experience where I grew both as a researcher and as a person.

Thank you to my advisory committee members, Dr. David Heinrichs and Dr. John McCormick. Their advice and feedback were greatly appreciated in the completion of this thesis.

I would like to acknowledge all past and present members of the McGavin lab for their support and friendship throughout my time in the lab, especially to the following members. To Heba Alnaseri and Jamie Halucha, I thank you for making my transition into the lab a very welcoming experience and for your guidance and encouragement while teaching me. To Robert Kuiack and Emily Xiong, thank you for fostering a wonderful and supportive work environment, for our fritter/Pokémon Go outings, and for making these past two years incredibly enjoyable ones.

Lastly, I would like to thank my friends and family for their unwavering support during my time in graduate school. It would not have been possible without them.

Table of contents

List of Tables

List of Figures

List of Abbreviations

Δ	Delta for deletion
Δ*fakA*	*fakA* deletion
Δ *farER*	*farER* deletion
AA	Arachidonic acid
ACME	Arginine catabolic mobile element
Agr	Accessory gene regulator
Amp	Ampicillin
ATP	Adenosine triphosphate
BLAST	Basic local alignment search tool
BSA	Bovine serum albumin
C	Cysteine
CA-MRSA	Community-acquired MRSA
Cm	Chloramphenicol
Cys	Cysteine
Dha	Dihydroxyacetone
DMSO	Dimethyl sulfoxide
DNA	Deoxyribonucleic acid
DTT	Dithiothreitol
EDTA	Ethylenediaminetetraaceticacid
EMSA	Electrophoretic mobility shift assay
Fak	Fatty acid kinase
FAME	Fatty acid modifying enzyme
FAR	Fatty acid resistance
FarE	Effector of fatty acid resistance
FarR	Regulator of fatty acid resistance
FarR7	FarR protein from the variant FAR7 clone
Gly	Glycine
H	Histidine
HA-MRSA	Hospital-associated MRSA
His	Histidine

IgG	Immunoglobin G
IPTG	Isopropyl 1-thio-β-D-galactopyranoside
IR	Inverted repeat
IRDye	Infrared Dye
Isd	Iron-regulated surface determinant
Km	Kanamycin
LA	Linoleic acid
LB	Luria Bertani
MRSA	Methicillin resistant *Staphylococcus aureus*
MSCRAMMs	Microbial surface components recognizing adhesive matrix molecules
NEB	New England Biolabs
OP	Operator site
OP_{farE}	FarR operator site; lies upstream of P_{farE}
OP_{farR}	FarR operator site; overlaps P_{farR}
OP_{PAL1}	FarR operator site; overlaps PAL1 and P_{farR}
P	Promoter
P_{farE}	*farE* promoter
P_{farR}	*farR* promoter
PAGE	Polyacrylamide gel electrophoresis
PAL	Pseudo-palindrome
PBP	Penicillin binding protein
PBS	Phosphate buffered saline
PCR	Polymerase chain reaction
PHYRE	Protein homology/analogy recognition engine
Pls	Phosphate acyltransferase
Poly[d(I-C)]	Poly-deoxyinosinic-deoxycytidylic acid
PtdOH	Phosphatidic acid
PVDF	Polyvinylidene difluoride
PVL	Panton-Valentine leucocidin
Qac	Quaternary ammonium antiseptic compounds
RBS	Ribosome binding site

RND	Resistance nodulation cell division
Sar	Staphylococcal accessory regulator
SCC*mec*	Staphylococcal cassette chromosome
Scz	Streptococcus zinc-sensing regulator
SDS	Sodium dodecyl sulfate
sRNA	small RNAs
TBE	Tris-borate-EDTA
TFR	TetR family transcriptional regulator
TSA	Tryptic soy agar
TSB	Tryptic soy broth
Tyr	Tyrosine
uFFA	Unsaturated free fatty acid
UTR	Untranslated region
UV	Ultraviolet
v/v	Volume/volume
w/v	Weight/volume
Y	Tyrosine

List of Units

bp	Nucleotide base pair
˚C	Degrees Celsius
Da	Dalton
g	Grams
xg	Force of gravity
k	Kilo
L	Litre
µ	Micro (10^{-6})
m	Milli (10^{-3})
M	Molar (1mol/L)
n	Nano (10^{-9})
OD	Optical density
Ω	Ohm
RPM	Revolutions per minute
V	Volts

1 Introduction

1.1 Overview of *Staphylococcus aureus*

1.1.1 Background

Staphylococcus aureus is a Gram-positive, spherical bacterium belonging to the Firmicutes phylum. The etymology of *S. aureus* describes the morphology of this species very well. The prefix derives from the ancient Greek "staphylē*"* for bunch of grapes, and describes the characteristic clusters it forms, while the species name derives from the Latin "aurum", describing its golden hue when grown on solid media. *S. aureus* exhibits duality in its nature as it colonizes approximately 30% of the population asymptomatically yet is able to cause mild to severe infections opportunistically. As such, it is classified as a pathobiont (1).

The preferred site of *S. aureus* colonization is the anterior nares, but it is also known to colonize the skin and other mucosal surfaces such as the throat, vagina, perineum, and axillae (2, 3). Nasal carriage of *S. aureus* is characterized by three distinct carriage groups, persistent carriers (20%), intermittent carriers (60%) and non-carriers (20%) (4, 5). The reported 30% of the general population that is colonized by *S. aureus* is composed of a mix of persistent and intermittent carriers (4). Persistent carriers differ from intermittent carriers in several ways. Persistent carriers usually only harbor one distinct strain of *S. aureus* over time, while intermittent carriers may carry different strains over time. Additionally, *S. aureus* is isolated in greater abundance from persistent carriers compared to intermittent carriers (6). Moreover, *S. aureus* can more often be isolated from different sites of the body in persistent carriers, other than the anterior nares (3). Therefore, colonization status is a determinant of the development of *S. aureus* infection, as persistent carriers are at a greater risk of developing an infection due to the increased pathogen burden (7). It has been shown that *S. aureus* infections often appear to be of endogenous origin (8). However, the mortality rate of *S. aureus* caused bacteremia has been shown to be greater in non-carriers than those who are colonized (9). Infections caused by *S. aureus* usually manifest as soft tissue infections and abscesses. However, it can also cause severe, and life-threatening complications such as endocarditis and osteoarticular infections.

1.1.2 Pathogenesis

S. aureus is able to infect virtually every tissue of the body due to the large variety of virulence factors at its disposal. Once the integrity of the epithelial barrier is compromised either through skin or hair follicle abrasions, surgery or indwelling medical devices, *S. aureus* is able to initiate infection by adhering to host factors using microbial surface components recognizing adhesive matrix molecules (MSCRAMMs). *S. aureus* encodes up to 20 MSCRAMMs that bind to host factors such as collagen, fibrinogen, and fibronectin (10). In order to survive within the host, *S. aureus* must additionally overcome nutritional immunity, by which the host sequesters vital nutrients to limit the proliferation of the invading pathogen. One example of nutritional immunity is the sequestration of iron. The majority of iron within mammals is located intracellularly, and the remainder is bound by high-affinity iron-binding proteins (11). One mechanism *S. aureus* uses to acquire iron is the secretion of siderophores, which have an extremely high affinity for iron, such that they are able to strip iron from host iron-binding proteins (12).

Initial infection of skin and soft tissue usually manifests as abscesses, from which the bacteria can disseminate to infect other tissues of the body. Although the formation of abscesses beings with localized recruitment of immune cells, *S. aureus* has many immune evasion mechanisms to thwart both the innate and adaptive immune system. To evade phagocytosis, *S. aureus* secretes chemotaxis inhibiting proteins and formyl peptide receptor-like 1 inhibitory protein, which both interfere with the chemotactic ability of neutrophils (13, 14). Moreover, staphylococcal protein A, a surface protein binds the Fc of immunoglobins, capturing the immunoglobin in the incorrect orientation needed to initiate phagocytosis through opsonization (15). In the event that phagocytosis does occur, *S. aureus* is able to evade killing by reactive oxygen species (ROS) via proteins such as catalase and superoxide dismutase (16). Furthermore, staphyloxanthin, the pigment that gives rise to the characteristic golden colour of *S. aureus*, has anti-oxidant properties, further contributing to protection against ROS (17). Finally, *S. aureus* secretes pore-forming toxins, such as Panton-Valentine Leukocidin (PVL), and α-toxin to kill neutrophils (18,19). Therefore, due to the large amount of immune cell lysis by *S. aureus*, the centre of abscesses contains an exudate of necrotic immune cells (20).

To disseminate from abscesses, global regulators such as *agr* can sense the population density of *S. aureus*. When the density is high, surface receptors for adhesion are downregulated while secreted effectors are upregulated. This allows *S. aureus* to leave the initial site of colonization and spread to other body tissues (21). An important secreted protein is α-toxin. As mentioned previously, α-toxin lyses neutrophils but also contributes to the dermonecrosis of abscesses through the lysis of erythrocytes, epithelial cells, and endothelial cells (22). Additionally, α-toxin activates a disintegrin and metalloprotease-10 (ADAM10), leading to subsequent proteolysis of E-cadherin. This results in the collapse of adherens junctions that connect epithelial cells to one another, allowing *S. aureus* to disseminate (22). *S. aureus* also secretes many additional tissue-degrading enzymes, including extracellular proteases. The staphylococcal proteolytic cascade is composed of the proteases aureolysin, SspA, and SspB and these proteases have been shown to degrade immunoglobin, complement, and elastin, an important protein of the extracellular matrix (23, 24). This pathway has also been found to be induced by unsaturated free fatty acids, which are present on the skin and within abscesses (25). Additional virulence factors of *S. aureus* include the superantigen toxic shock syndrome toxin-1, (26). These molecules force non-specific activation of T-cells, leading to a massive release of cytokines. This cytokine storm can cause toxic shock syndrome. Finally, *S. aureus* is able to form biofilms in which they are protected from immune cells and antibiotics. Biofilms are often formed on indwelling medical devices, causing chronic infections in these patients (27).

1.1.3 Emergence of antibiotic resistance

Before the advent of penicillin, bacteremia caused by *S. aureus* had a mortality rate of between 75-83% (28). Therefore, the discovery of penicillin in 1928 by Sir Alexander Fleming was revolutionary for modern medicine, and for this discovery, he was awarded a Nobel prize. Penicillin functions by binding transpeptidases/penicillin-binding proteins (PBPs) that are responsible for crosslinking the peptidoglycan of the cell wall. However, in 1942, a few years after the clinical introduction of penicillin, resistant strains of *S. aureus* began to emerge (29). These strains produced penicillinase, a β-lactamase which hydrolyses the active β-lactam ring of penicillin, rendering it ineffective. Methicillin, a penicillinase-resistant β-lactam antibiotic was later introduced, but once again, methicillin-resistant strains arose soon after its introduction.

Horizontal gene transfer with *Staphylococcus epidermidis*, a commensal skin bacterium, lead to the acquisition of the SCC*mec* cassette, which contains the gene *mecA*. *mecA* encodes for PBP2, a PBP with lower affinity for β-lactams (30). The acquisition of *mecA* not only renders MRSA resistant to methicillin but all other β-lactam derived antibiotics: penicillins, cephalosporins, and carbapenems. Until the 1990s, these strains of MRSA were largely confined to the hospital setting (HA-MRSA), causing nosocomial infections. HA-MRSA strains usually harbor SCC*mec* types I, II, and III, which also carry resistance genes for multiple antibiotics such as kanamycin, neomycin, tetracycline, and erythromycin (29).

However, in the early 90s, these MRSA strains were found in the community in healthy patients who had not had prior exposure to a healthcare setting and were termed community-acquired MRSA (CA-MRSA). CA-MRSA usually harbor *SCCmec* type IV, V, and VI. In contrast to the SCC*mec* types harboured by HA-MRSA, types IV, V and VI, do not carry multi-drug resistance, and only carry resistance to β-lactam derivatives (31). However, types IV, V, and VI are much smaller in size than types I, II, and III, giving a fitness advantage in the absence of antibiotics (32). Since the 90s, CA-MRSA of multiple lineages has been found on every continent. USA300 is the predominant CA-MRSA strain found in North America and is the primary cause of skin and soft tissue infections in the United States (33). Although initially only resistant to β-lactam antibiotics, resistance to other antibiotics such as macrolides and fluoroquinolones have also developed. Additionally, reduced susceptibility to vancomycin and daptomycin in USA300 isolates has also been found (34).

1.2 USA300 virulence

1.2.1 Origins and spread of USA300

Before the introduction of multilocus sequence typing (MLST) and staphylococcal protein A (*spa*) typing, pulse-field gel electrophoresis (PFGE) was used to identify isolates of *S. aureus.* USA300 was first identified through this method, along with 8 other initial MRSA strains (USA100-800) isolated from the United States (35). USA300 emerged from *S. aureus* MLST 8, which is the presumptive ancestor of MRSA and the first to acquire the SCC*mec* cassette. Furthermore,

USA300 is speculated to have arisen from USA500, a strain of HA-MRSA, and differs from its ancestor by several unique genomic features that render it particularly more aggressive and hyper-virulent than other strains of CA-MRSA. USA300 harbors SCC*mec* type IV (36), and other accessory genetic elements found in the USA300 genome include PVL, enterotoxins *sek2* and *seq*2, and the arginine catabolic mobile element (ACME), the latter being unique to USA300 (37). PVL is a bacteriophage-encoded β-pore toxin that lyses neutrophils, monocytes, and macrophages, causing subsequent tissue necrosis through the release of inflammatory cytokines (31).

USA300 was first found only in North America, while other continents had their own predominant strain of MRSA. The first known cases caused by USA300 were found in football players in Pennsylvania and later was found to be responsible for an outbreak of soft tissue infections in prison inmates in Mississippi (37). It was later found in other states in patients who had no prior exposure to a healthcare setting. USA300 is now found across the globe in 36 countries across 5 continents, including North America, Colombia, Australia, Japan, Israel, which can be explained in part due to increased international travel (38). In Canada, USA300 has been the predominant strain of CA-MRSA since 2004 (39, 40).

1.2.2 Evasion of skin innate immune defenses

The human skin is an interface between the host and the environment, and therefore, the first line of defence against invading pathogens. Not surprisingly, the skin has many immune defence mechanisms to limit colonization and infection. Firstly, the tightly linked corneocytes of the stratum corneum represent a physical barrier to invading pathogens (41). Skin also has a low moisture content and is at a lower temperature than the rest of the body, which slows the replication of pathogens (42). Chemical barriers are also secreted from the skin, including lysozyme, antimicrobial peptides, and sebum. Antimicrobial peptides are small, charged peptides secreted by keratinocytes that insert themselves into bacterial membranes, creating pores and disrupting membrane integrity. Keratinocytes upregulate antimicrobial peptide production in response to the wounding of the epithelial barrier or during infection (42).

Human skin is coated by a lipid mixture, secreted by the sebaceous glands in the dermis of the skin. It is composed of squalene, wax monoesters, cholesterol, cholesterol esters, and triglycerides. The triglycerides are hydrolyzed by lipases secreted by the flora of the skin, and by an acid lipase released by the lamellar granules of keratinocytes, releasing free fatty acids, giving the skin an acidic pH (43). Sapienic acid (C16:1) and oleic acid (C18:1) are the main uFFAs to originate from sebum, while linoleic acid (C18:2) and arachidonic acid (C20:4) are found in nasal secretions (44). *S. aureus* is also exposed to linoleic acid during the context of infection, mainly in abscesses (45). To exert their toxic effects on bacteria, free fatty acids are thought to enter the cell through passive diffusion and cause subsequent disruption of membrane integrity, leading to an influx of H^+ ions and leakage of metabolites, affecting oxidative phosphorylation (46). Additionally, those with deficiencies in uFFA production are more susceptible to skin infections caused by *S. aureus* (47). Arachidonic acid also has a role in the oxidative burst produced by macrophages and neutrophils. In this inflammatory burst, arachidonic acid is autoxidized by ROS to various electrophilic molecules, including free aldehydes, α,β-unsaturated carbonyls and isolevuglandins (48). These reactive electrophiles damage the cellular machinery of *S. aureus,* leading to cell death.

The success of USA300 can be attributed, in part, in its ability to overcome these innate immune defenses. Part of this is attributed to the acquisition of the arginine catabolic mobile element (ACME) through horizontal gene transfer with *Staphylococcus epidermidis,* a commensal skin bacterium (49). Arginine is an important mediator in the cutaneous immune response as it is responsible for both initial inflammation and eventual resolution. Additionally, during the onset of inflammation, arginine is metabolized to produce NO•. During the resolution of inflammation, arginine is converted to ornithine, which is subsequently converted to polyamines. Polyamines are necessary to promote proper tissue repair during wound healing. They are also toxic to *S. aureus* at physiological concentrations. ACME contains the *arc* operon, which encodes the arginine deiminase pathway genes. These genes catalyze the conversion of arginine to ornithine, as well as ATP and ammonia, which is important as to deacidify the skin. However, ornithine is produced in this reaction and is subsequently converted to toxic polyamines. To mitigate this issue, ACME also encodes *speG*, a polyamine acetyltransferase that confers polyamine resistance to USA300 (50).

1.2.3 Resistance to antimicrobial fatty acids

S. aureus employs three main mechanisms in which to protect against antimicrobial fatty acids; modification of cell wall molecules and phospholipid bilayer, efflux pumps, and metabolic detoxification. Upon exposure to antimicrobial fatty acids, *S. aureus* upregulates genes for carotenoid biosynthesis. Carotenoids are lipophilic and can be inserted into the phospholipid bilayer where, they increase the stability of the membrane (51). Staphyloxanthin, the carotenoid which gives *S. aureus* its golden hue, is involved in this process as studies have shown a positive correlation between pigment and resistance to oleic acid (52). IsdA is a surface protein and adhesion factor that binds to fibrinogen, fibronectin and transferrin, and is required for nasal colonization. However, IsdA has also been shown to mediate resistance to antimicrobial fatty acids. The C-terminal tail of IsdA is anchored to the cell membrane. When IsdA expression is upregulated, the hydrophobicity of the membrane decreases, thereby rendering the membrane less susceptible to bactericidal fatty acids (53). Moreover, wall teichoic acid also confers resistance to antimicrobial fatty acids. Wall teichoic acids are necessary for nasal colonization and are believed to confer a high charge to the cell wall, thereby repelling antimicrobial fatty acids (54). *S. aureus* also encodes efflux pumps in which to remove antimicrobial fatty acids once present in the cytoplasm. Tet38, a tetracycline efflux pump, also removes palmitoleic acid from the bacterial cell (55). Additionally, our lab has previously discovered *farE*, a RND-family efflux pump that promotes efflux of arachidonic acid and linoleic acid (56). Finally, *S. aureus* is also able to metabolically detoxify antimicrobial fatty acids. Fatty acid modifying enzyme (FAME) detoxifies bactericidal fatty acids found in abscesses through their esterification to various alcohols (57). Moreover, host-derived fatty acids can also be incorporated into phospholipid by fatty acid kinase FakA and FakB1/2 (58).

1.3 Fatty acid machinery of *Staphylococcus aureus*

1.3.1 Phospholipid composition and synthesis

The phospholipid bilayer of *S. aureus* is mainly comprised of three types of polar lipids, phosphatidylglycerol, lysyl-phosphatidylglycerol, and cardiolipin (59). To maintain homeostasis of the membrane, many organisms adjust the ratio of saturated to unsaturated fatty acids, making the membrane more rigid and fluid, respectively. However, unlike many other bacteria such as *Bacillus subtilis*, *S. aureus* does not encode desaturase enzymes, meaning that it is unable to produce unsaturated fatty acids (60). Therefore, to regulate the fluidity of its membrane, *S. aureus* also synthesizes both straight-chain and branched-chain fatty acids. Branched-chain fatty acids (BCFA) are synthesized from the branched-chain amino acids (BCAA) leucine, valine, and isoleucine, the latter of which gives the most membrane fluidity (61). As much as 55% of phospholipids that make up the membrane in *S. aureus* are derived from BCFA (62). BCAA are transaminated by the enzyme branched-chain amino acid transaminase (BAT), giving rise to branched-chain α-keto acids (62). These branched-chain α-keto acids are then decarboxylated by α-keto acid dehydrogenase producing branched-chain acyl coenzyme A derivatives. In a series of reactions performed by the fatty acid biosynthetic (Fab) proteins of the FASII cycle, the branched-chain acyl coenzyme A derivatives are elongated to produced long-chain acyl-acyl carrier protein (ACP) (59). These long chain acyl-ACPs then feed into the remainder phospholipid synthesis, which, in many Gram-positive bacteria, is carried out by the PlsXYC acyltransferase system. PlsX, a peripheral membrane protein, catalyzes the transfer of the acyl group of long-chain acyl-ACP to acyl-phosphate. PlsY then transfers the acyl group to glycerol-3-phosphate (G3P). Finally, PlsC transfers a second fatty acid group to the acyl-G3P, creating phosphatidic acid (PtdOH), which is the main intermediate of phospholipid synthesis in eubacteria. PtdOH can then be used to synthesize phosphatidylglycerol, leading to the synthesis of lysyl-phosphatidylglycerol, cardiolipin, and lipoteichoic acids. Deletion of *plsY* is lethal to *S. aureus;* however, when *plsX* is deleted, the resulting strains are fatty acid auxotrophs (60, 64).

1.3.2 Incorporation of exogenous fatty acid into phospholipids

It is unknown whether *S. aureus* is able to use host-derived fatty acid as an energy source through β-oxidation. However, *S. aureus* does possess another mechanism in which to utilize and de-toxify exogenous fatty acids simultaneously. Additionally, the synthesis of both straight and branched-chain fatty acids is energetically expensive, and it would be optimal for *S. aureus* to make use of the exogenous fatty acids found in the environment. Both saturated and unsaturated exogenous fatty acids enter the cell through passive diffusion and by the pH gradient, are flipped to the inner leaflet of the membrane. Once in the cell, saturated and unsaturated fatty acids are bound by the fatty acid binding protein FakB1 and FakB2, respectively. Once bound by FakB1/2, they are phosphorylated by the ATP-dependent fatty acid kinase FakA, creating an acyl-phosphate. The resulting acyl-phosphate can either be converted to acyl-ACP to be extended through FASII machinery or directly incorporated into phospholipid by the PlsXYC acyltransferase system, producing phosphatidic acid, which can then be used to synthesize phosphatidylglycerol, lysyl-phosphatidylglycerol, cardiolipin and lipoteichoic acids (Fig 1.1). However, eventually the buildup of uFFA surpasses the rate of membrane incorporation by FakA and the PlsXYC acyltransferase system and will lead to cell death (46, 54).

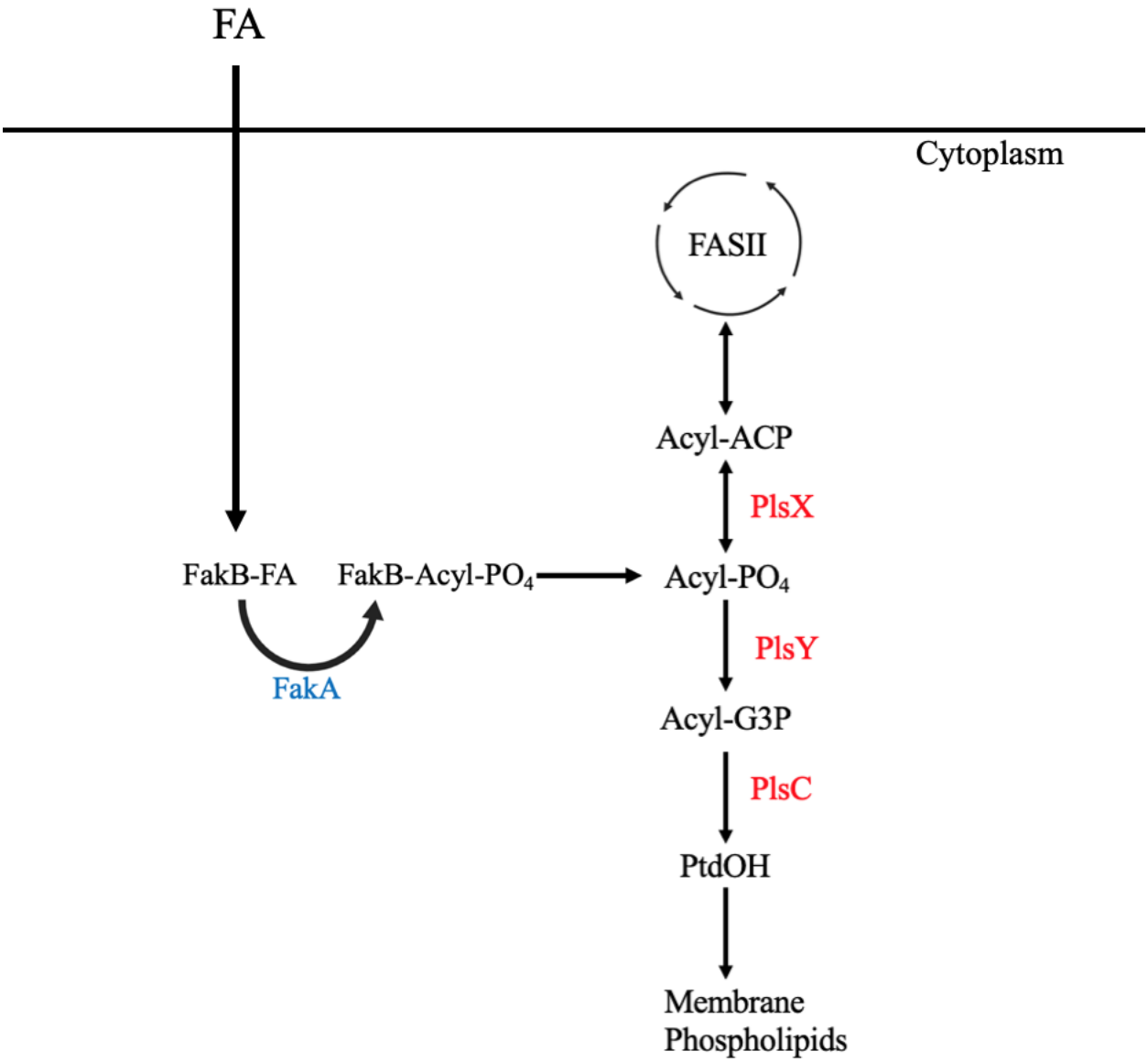

Figure 1.1 Incorporation of exogenous fatty acid into membrane phospholipids in S. aureus Upon entry into the cell, exogenous fatty acids (FA) are bound by FakB and subsequently phosphorylated by FakA. Phosphorylated fatty acids can either be extended by the FASII machinery or can directly incorporated into membrane phospholipid. Figure adapted from Kuhn *et al.* (59).

1.4 Resistance-nodulation division family transporters

Efflux pumps are commonly found in many bacterial species and represent important mediators of antibiotic resistance. There are currently five defined classes of efflux pumps: the major facilitator superfamily, the ATP-binding cassette superfamily, the small multidrug resistance superfamily, the multidrug and toxic compound extrusion superfamily and the resistance-nodulation division-superfamily (RND). RND family efflux pumps are able to transport a wide range of substrates, including small hydrophobic compounds, metals, and antibiotics. The majority of our knowledge of RND family efflux pumps comes from research done in Gram-negative bacteria, and although RND family efflux pumps are present in Gram-positive species, they have been less well characterized in these bacteria. A well-characterized RND family efflux pump is the multidrug efflux AcrA-AcrB-TolC complex in *E. coli*, of which AcrB is an RND family efflux pump that interacts with AcrA and TolC to form a tripartite complex. ArcB and TolC are transmembrane proteins in the inner and outer membrane, respectively, and AcrA bridges the two in the periplasm, creating a continuous channel to allow efflux of a substrate, which are typically hydrophobic antibiotics or bile salts (55, 56). Although Gram-positive bacteria and Mycobacterium species do not have an outer membrane, they still encode RND family efflux pumps that bear homology to AcrB in *E. coli*, for example, MmpL in *Mycobacterium tuberculosis* which transports lipids to the cell wall (67). *S. aureus* encodes three RND-family efflux pumps, including FemT, which is thought to be involved in cell wall synthesis, SecDF, which plays a role in protein secretion, and FarE which promotes efflux of uFFA (44, 56, 57).

1.5 TetR family transcriptional regulators

Bacteria use signal transduction systems to sense the environment around them to properly regulate gene expression of antibiotic resistance genes and to maintain homeostasis of important biochemical processes. Of these signal transduction systems, there are two main types; one-component and two-component signal transduction systems. One-component signal transduction systems operate using one protein that is responsible for both the sensing of the environment and gene regulation, whereas in the two-component system, the sensing and gene regulation is done by different proteins (70).

The TetR family of transcriptional regulators (TFR) is a group of one-component signal transduction systems found in many species of bacteria. There are over 2500 known TFRs that are responsible for a wide variety of functions, including antibiotic resistance, cell-cell signalling and the metabolism of lipids, amino acids, and nitrogen. TFRs have an α-helical structure, with helix-turn-helix DNA binding domains that usually bind palindromic DNA sequences. The majority of TFRs are known to be autoregulatory. Additionally, most of these regulators function to repress their target gene, although some TFRs are known to be activators, as well as some functioning as both repressor and activator (70–72). The DNA binding affinity of TFRs is also modulated after binding a small molecule ligand, and in the case of a TFR regulating an efflux pump, the ligand is usually the substrate of the efflux pump. All TFRs consist of an N-terminal DNA-binding domain and a C-terminal domain that usually binds a ligand. The ligand-binding domain has the ability to alter the DNA binding affinity of the N-terminal domain once bound to a ligand. TFRs usually function as dimers; however, some members of this family may also function as tetramers or through other oligomerization states. TFRs can also be further categorized into three subgroups depending on the position and orientation of the gene encoding the regulator to that of the effector protein. In type one TFRs, the TFR is divergently transcribed from the regulated target gene, and this group makes up the majority of TFRs. The prototypic TFR, TetR is found in *E. coli* and is responsible for regulating *tetA,* which encodes a tetracycline efflux pump, promoting resistance to tetracycline. TetR is a type-1 TFR, and as such, it is divergently transcribed from *tetA* and functions as a repressor of transcription. In the absence of its ligand, tetracycline, the TetR homodimer remains bound to overlapping operator sequences in the intergenic segment, repressing the transcription of both *tetR* and *tetA*. When tetracycline enters the cell, it is bound by TetR, causing a conformational change in the protein in which it is unable to bind to the intergenic operator sites, promoting the expression of both *tetR* and *tetA* (73).

However, there are many TFRs that, in part, deviate from the typical paradigms of TFR function. An example of this is DhaS in *Lactococcus lactis* in which dihydroxyacetone metabolism is regulated in a mechanism consisting of co-activator proteins. DhaQ binds the physiological ligand dihydroxyacetone. The DhaQ-dihydroxyacetone complex then binds to DhaS, a member of the TetR family. Only when DhaS binds the DhaQ-dihydroxyacetone complex is it able to activate the

expression of genes required for dihydroxyacetone metabolism. DhaS is also an unconventional TFR in the respect that it is a transcriptional activator and not a repressor (74).

TFRs can be found in *S. aureus* as well. QacA is a multi-drug efflux pump for quaternary ammonium-type antiseptic compounds and is negatively regulated by the TFR QacR. QacR does not bind to the promoter of *qacA*, which is unusual of TFRs. However, it does bind to an inverted repeat located downstream of the *qacA* promoter. The binding of this inverted repeat may still allow RNA polymerase to bind, but it would prevent the transcriptional machinery from being able to fully access the gene. Both *qacA* and *qacR* are accessory genetic elements, encoded for on the pSK616 plasmid (75–77). IcaR is a TFR in *S. aureus* that is chromosomally encoded. IcaR regulates the *icaADBC* operon that is responsible for the biosynthesis of poly-N-acetlyglucosamine for the formation of biofilms. IcaR represses the transcription of the *icaABDC* operon through the binding of a TATTT motif. However, IcaR has not been shown not to be involved in autorepression (68, 69). Finally, FarR another TFR in *S. aureus* regulated the RND family, unsaturated free fatty acid efflux pump FarE. FarR is unusual in the sense that it both represses and activates *farE* (56).

1.6 FarE and FarR

1.6.1 Overview of FarE and FarR

S. aureus can detoxify and utilize uFFA by incorporating them into the phospholipid bilayer through the FakA/B, and PlsXYC acyltransferase system. There are also other methods by which *S. aureus* can increase their resistance to uFFA. For example, resistance to palmitoleic acid can be conferred through several methods. Teichoic acids can restrict the access of palmitoleic acid to the cytoplasmic membrane (54). *S. aureus* also encodes *tet38,* a major facilitator superfamily efflux pump that promotes efflux of palmitoleic acid out of the cell (80). However, both of these methods only promote resistance to palmitoleic acid. Our lab has found another mechanism by which *S. aureus* can detoxify and increase their resistance to other uFFAs. We have previously identified *farE* (SAUSA300_2489) and *farR* (SAUSA300_2490), a divergently transcribed regulator and effector pair in USA300. *farE* encodes an 822 amino acid, 90.4kDa RND-family efflux pump that promotes efflux of fatty acids, the expression of which can be induced by linoleic and arachidonic

acid (56). *farR* encodes a 182 amino acid 21.9 kDa type-1 TFR with an N-terminal DNA binding domain that is responsible for regulating *farE.* FarE and FarR are homologous to RND-family efflux pump AcrB and its regulator AcrR a TFR, respectively. Genome annotations also assign FarE to the MmpL family of proteins from *Mycobacterium tuberculosis* (81). FarE expression is tightly regulated and is only expressed when induced by uFFA, with higher levels of induction when exposed to arachidonic acid and linoleic acid, which are commonly found in the anterior nares compared to sapienic acid which is found in sebum.

1.6.2 Features of the *farER* intergenic segment

As *farR* and *farE* are divergently transcribed, both of their promoters lie within the 144 nucleotide long intergenic segment (Fig 1.2), and previous experiments in our lab have identified three operator sites within: O_{farE}, O_{farR}, and O_{PAL1} (82). O_{farE} lies upstream of the *farE* promoter (P_{farE}) and is situated in a position that would be consistent with a role in activation of *farE* expression. P_{farE} also has high GC content, which is indicative that a transcriptional activator is needed, especially considering that *S. aureus* has high AT content. O_{farR} overlaps with the promoter of *farR* (P_{farR}) and is downstream of the +1 transcription start site of *farE*, while O_{PAL1} bridges the +1 transcription start sites of P_{farR} and P_{farE} and overlaps with O_{farR}. Both the positions O_{PAL1} and O_{farR} would be consistent with a role in autorepression. TFRs usually bind to palindromic repeats as operator sites, and our lab has previously identified two pseudo-palindromic repeats within the intergenic segment. PAL1 spans the transcriptional start site of both *farR* and *farE* and is located within O_{PAL1} while PAL2 is located upstream of P_{farE} and is located within O_{farE}. Additionally, the inverted repeats of PAL1 and PAL2 are juxtaposed. All three operator sites also share a conserved sequence of TAGWTTA with a TAG sequence central to each operator. This sequence can be found in both pseudo-palindromes and also in O_{farR} where it overlaps with the -10 promoter element TATAGT of P_{farR}.

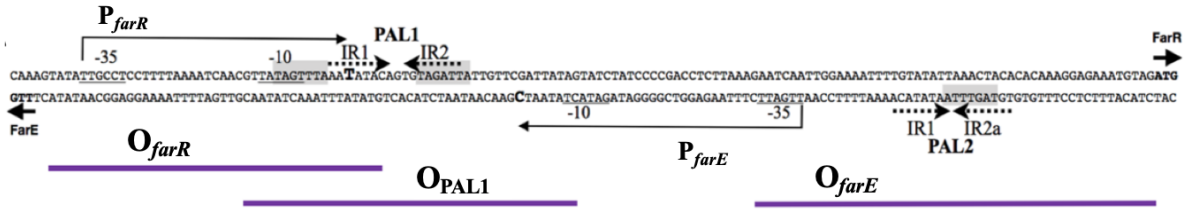

Figure 1.2 Intergenic segment of *farER*. The *farER* intergenic segment is 144nt long with three FarR operator sites within. O_{farR} overlaps the -10 element of P_{farR}, O_{farE} lies downstream of P_{farE}, and O_{PAL1} lies in between. Inverted repeats (IR1, IR2, IR2a) that comprise the pseudopalindromes (PAL1 and PAL2) are also labeled. Shaded nucleotides highlight a conserved TAGWTTA motif that is common to each operator site. Figure adapted from Alnaseri *et al.* (82).

1.6.3 Regulation of *farE* by FarR

FarR tightly regulates the expression of FarE, which may be to limit the sustained efflux of resources or endogenously synthesized straight and branched-chain fatty acids. FarR is a type-1 46TFR, and as such, it is divergently transcribed from *farE* and also expected to repress *farE* expression. However, FarR deviates from the typical paradigms of TFRs as it is required for the activation of *farE* as it was found that in a *farR* transposon mutant, *farE* was unable to be induced (56). It was also found that *farR* is subject to autorepression, as typical for a TFR. Of the three possible operator sites, both O_{farR} and O_{PAL1} would be consistent with a role in autorepression, and we have demonstrated that a G>A point mutation in the TAGWTTA motif of O_{farR} causes de-repression of FarR (82).

Previous studies in our lab have also identified a fatty acid resistant clone of USA300 (FAR7) that has a single nucleotide polymorphism that corresponds to a $H_{121}Y$ substitution in *farR* (hereafter referred to as *farR7*). The FAR7 clone exhibits greater resistance to uFFA as it can no longer bind O_{farR}, causing de-repression of *farR*, and subsequently increased activation of *farE*. FarR7 has also been shown to interact well with O_{farE} (44, 71). However, this $H_{121}Y$ substitution does not lie in the N-terminal DNA binding domain, but in the C-terminal ligand-binding domain. It is proposed that this $H_{121}Y$ amino acid substitution allows FarR7 to mimic ligand-bound conformation,

allowing FarR7 to better bind to activating operator sites to increase expression of FarE and subsequent resistance to uFFA.

A defining characteristic of TFRs is that they typically bind a small molecule ligand that modifies DNA binding. There are reports of other TFRs that bind acyl-CoA, and although arachidonic acid and linoleic acid are the strongest known inducer of *farE* expression, their acyl-CoA derivatives have been shown not to modify FarR DNA binding (82–84). In addition to FarE, the incorporation of exogenous fatty acids into membrane phospholipids by FakA and FakB1/2 is another mechanism by which *S. aureus* utilizes to overcome antimicrobial fatty acids. However, there may an interplay between FakA and FakB1/2 and FarR and FarE. We have previously determined that in USA300Δ*fakA*, *farE* exhibits an increased basal level of transcription, but cannot be fully induced (82). As FakA catalyzes the formation of acyl-phosphates, these findings suggest that the presence of such acyl-phosphates may modify FarR function. It has also been reported that non-esterified fatty acids accumulate within the cytosol of USA300Δ*fakA*, which may explain the increased basal level of transcription and the inability to be fully induced (85).

1.7 Hypothesis and Rationale

The goal of this work was to address the nucleotide binding and sensor specificity of FarR. We have previously shown that mutation in the common TAGWTTA motif of O_{farR} relieves autorepression. However, the role of the conserved TAGWTTA motif in O_{PAL1} and O_{farE} have not been identified. Due to the position of $O_{PAL1,}$ we hypothesize that the mutation of this motif or mutation of PAL1 will lead to de-repression of *farR*, similar to the de-repression of *farR* when a G>A mutation was introduced into the TAGWTTA motif of O_{farR}. We further hypothesize that the de-repression of *farR* through either mutation will lead to an increased activation of *farE* expression, and subsequent increased resistance to linoleic acid, as seen in the FAR7 variant. Additionally, we hypothesize that mutations in the TAGWTTA motif of O_{farE} will interfere with FarR binding, leading to decreased resistance to linoleic acid.

Furthermore, the role of amino acid substitutions in FarR will be examined, specifically, the role of cysteine residues in FarR function. FarR contains two cysteine residues, C37 within the N-terminal DNA binding domain and C116 within the C-terminal ligand-binding domain. Cysteine residues are able to sense changes in the local redox environment of the cell. Arachidonic acid released from the oxidative burst of immune cells has been shown to kill *S. aureus* through a lipid peroxidation mechanism, creating an oxidative environment in the cell. As arachidonic acid as shown to be the strongest inducer of *farE* expression, we hypothesize that both cysteine residues are important for FarR function.

The sensor specificity of FarR also remains to be determined. A defining characteristic of TFRs is that they typically bind a small molecule ligand that modifies DNA binding affinity, and several pieces of our data indicate that FarR does the same. FarR7 has previously shown to interact well with O_{farE}, a proposed site of activation. The $H_{121}Y$ substitution of FarR7 is located in the C-terminal ligand-binding domain of the protein; however, the N-terminal domain is involved in DNA recognition and binding, which may indicate that this substitution changes the conformation of the protein as to mimic a ligand-bound state, allowing it to interact with PAL2. In USA300Δ*fakA*, the basal level of *farE* expression is increased, which may be due to an increased cellular pool of unphosphorylated fatty acids; however, *farE* is unable to be fully induced (82). From these observations, we hypothesize that the physiologic ligand of FarR is acyl-phosphates and that the binding of FarR to its ligand will modulate the DNA binding affinity allowing FarR to activate *farE* through PAL2. Another possibility is that FarR requires a co-activator protein, which may include FakA or FakB2, similar to DhaS and DhaQ in *L. lactis*. This work aims to shed light on the mechanisms by which *S. aureus* is able to overcome the innate defences of the skin and to colonize humans which may lead to insights on new therapeutic targets that can prevent colonization and subsequent infection.

2 Materials and Methods

2.1 Storage and growth of strains

A list of bacterial strains used or constructed in this study are provided in Table 2.1. Cultures were maintained as frozen stocks (-80°C) in tryptic soy broth (TSB) and 20% glycerol. To generate single colonies, *S. aureus* strains were streaked onto tryptic soy agar (1.5% Agar) plates supplemented with chloramphenicol (5 μg/mL) when required for plasmid maintenance. *E. coli* strains were grown on Luria Bertani (LB) agar or broth supplemented with ampicillin (100 μg/mL), kanamycin (50 μg/mL), or chloramphenicol (100 μg/mL) when required. Overnight cultures were generated by inoculating a single colony into a 13 mL polypropylene tube containing 3mL of media supplemented with antibiotic when needed and grown at 37°C with shaking at 220 rpm for 18 hours.

Table 2.1 Strains and plasmids used in this study

Strain or Plasmid	Description[a]	Source or reference
Strains:		
S. aureus:		
RN4220	r_{K^-} m_{K^+}; capable of accepting foreign DNA	(86)
USA300	CA-MRSA, wild-type strain cured of resistance plasmids	(25)
FAR7	Fatty acid resistance clone 7, single nucleotide polymorphism H121Y in *farR*	(56)
USA300Δ*farER*	USA300LAC with markerless deletion of *farE* (SAUSA300_2489) and *farR* (SAUSA300_2490)	(82)
USA300Δ*farER* (pLI50)	USA300ΔfarER with pLI50; Cm^r	(82)
USA300Δ*farER* (pLI*farER*)	USA300ΔfarER complemented with pLIfarER; Cm^r	(82)
USA300Δ*farER* (pLI*farER*1)	USA300ΔfarER complemented with pLIfarER1; Cm^r	(82)

USA300Δ*farER* (pLI*farER*2)	USA300ΔfarER complemented with pLIfarER2; Cm^r	(82)
USA300Δ*farER* (pLI*farER3*)	USA300ΔfarER complemented with pLIfarER3; Cm^r	(82)
USA300Δ*farER* (pLI*farER* PAL2)	USA300ΔfarER complemented with pLIfarER PAL2; Cm^r	This study
USA300Δ*farER* (pLI*farER*$_{ATG>TAG)}$	USA300ΔfarER complemented with pLIfarER$_{ATG>TAG}$; Cm^r	This study
USA300Δ*farER* (pLI*farER*$_{C37A}$)	USA300ΔfarER complemented with pLIfarER$_{C37A}$; Cm^r	This study
USA300Δ*farER* (pLI*farER*$_{C116A}$)	USA300ΔfarER complemented with pLIfarER$_{C116A}$; Cm^r	This study
M0049	Clinical isolate, isolated from sputum; FarR C116Y	(87)
M0330	Clinical isolate, isolated from unknown location; FarR C116Y	(88)
M0390	Clinical isolate, isolated from sputum; FarR C116Y	(89)
M0398	Clinical isolate, isolated from wound; FarR C116Y	(90)
M0423	Clinical isolate, isolated from bronchial washings; FarR C116Y	(91)
M1545	Clinical isolate, isolated from nares; FarR C116Y	(92)
E. coli:		
DH5α	λ^- ϕ80d*lacZ*ΔM15 Δ(*lacZYA-argF*)*U169 recA1 endA1 hsdR17*(r_K^- m_K^-) *supE44 thi-1 gyrA relA1*	Invitrogen
BL21 (DE3)	F^- *ompT gal dcm lon hsdSB* (r_B^- m_B^+) λ (DE3 [*lacI* l*acUV5*-T7 gene 1 *ind1 sam7 nin5*])	Novagen
M15[pREP]	F^-, Φ80ΔlacM15, thi, lac^-, mtl^-, *recA*$^+$, Km^r	Qiagen

Plasmids:		
pLI50	*E. coli – S. aureus* shuttle vector; Amp^R, Cm^R	(93)
pLI*farE*	pLI50 with *farE* expressed from native promoter; Amp^R, Cm^R	(56)
pLI*farR*	pLI50 with *farR* expressed from native promoter; Amp^R, Cm^R	(56)
pLI*farR7*	pLI50 with *farR* gene from variant FAR7 clone; Amp^R, Cm^R	(56)
pLI*farR*1	Mutagenesis of pLI*farR* with primers farR1-P and farR1-M primers; G>A substitution in -10 motif of P_{farR}; Amp^R, Cm^R	(82)
pLI*farR*2	Mutagenesis of pLI*farR* with primers farR2-P and farR2-M; nucleotide substitutions in PAL1; Amp^R, Cm^R	(82)
pLI*farR*3	Mutagenesis of pLI*farR*1 with primers f*arR*3-P and farR3-M; Amp^R, Cm^R	(82)
pLI$farR_{C37A}$	Mutagenesis of pLI*farR* with primers *farR* C37A-F and *farR* C37A-R; Amp^R, Cm^R	This study
pLI$farR_{C116A}$	Mutagenesis of pLI*farR* with primers *farR* C116A-F and C116A-R; Amp^R, Cm^R	This study
pLI$farR_{C116Y}$	Mutagenesis of pLI*farR* with primers *farR* C116Y-F and *farR* C116Y-R; Amp^R, Cm^R	This study
pLI$farR_{ATG>TAG}$	Mutagenesis of pLI*farR* with primers *farR* ATG>TAG-F and *farR* ATG>TAG-R; Amp^R, Cm^R	This study
pLI*farER*	*farE* excised from pLIf*arE* with KpnI-SacII, and ligated into KpnI-SacII digested pLI*farR*.; Amp^R, Cm^R	(56)
pLI*farER*1	As for pLI*farER*, except that the KpnI-SacII fragment was ligated into pLI*farR*1; Amp^R, Cm^R	(82)
pLI*farER*2	As for pLI*farER*, except that KpnI-SacII fragment was ligated into pLI*farR*2; Amp^R, Cm^R	(82)
pLI*farER*3	As for pLI*farER*, except that KpnI-SacII fragment was ligated into pLI*farR*3; Amp^R, Cm^R	(82)

pLI*farER*4	As for pLI*farER*, except that KpnI-SacII fragment was ligated into pLIf*arR*4; Amp^R, Cm^R	This study
pLI*farER*$_{ATG>TAG}$	As for pLI*farER*, except that KpnI-SacII fragment was ligated into pLIf*arR*$_{ATG>TAG}$; Amp^R, Cm^R	This study
pLI*farER*$_{C37A}$	As for pLI*farER*, except that KpnI-SacII fragment was ligated into pLIf*arR*$_{C37A}$; Amp^R, Cm^R	This study
pLI*farER*$_{C116A}$	As for pLI*farER*, except that KpnI-SacII fragment was ligated into pLIf*arR*$_{C116A}$ Amp^R, Cm^R	This study
pBAD33	*E. coli* vector, arabinose inducible; Cm^R	(94)
pBAD*fakAB2*	Native *fakA* and *fakB2* genes cloned in SacI and XbaI sites of pBAD33; Cm^R	This study
pQE30	*E. coli* vector for expression of N-terminal 6His-tagged fusion proteins; Amp^R	Qiagen
pQE*farR*	*farR* open reading frame amplified from USA300 with primers 6H*farR*-F and 6H*farR*-R, cloned at SacI and HindIII sites of pQE30; Amp^R	(56)
pQE*farR7*	As for pQE-FarR, except that template DNA was from S. aureus FAR7; Amp^R	(56)
pQE*farE-PD*	Amplified from USA300 with primers, cloned at BamHI and SalI sites of pQE30 ; Amp^R	This study

[a]Abbreviations: Amp^r – ampicillin resistance, Cm^r – chloramphenicol resistance, Km^r –kanamycin resistance

2.2 DNA Methodologies

2.2.1 Plasmid Isolation from *E. coli*

All plasmids used in this study are provided in Table 2.1. Plasmid DNA from *E. coli* was isolated using the Presto™ Mini Plasmid Kit (Geneaid) following the manufacturer's guidelines. Briefly, 3 mL of *E. coli* at stationary phase were pelleted via centrifugation in a microcentrifuge tube and then resuspended in 200 μL Solution I (50 mM Tris, pH 8.0, 20 mM EDTA, 100μg/mL RNaseA). Cells were then lysed through the addition of 200 μL Solution II (200 mM NaOH, 1% w/v SDS) and then incubated for 2 minutes at room temperature. The solution was then neutralized by the addition of 300 μL Solution III (guanidine hydrochloride with acetic acid) and inverted several times until a precipitate formed. Samples were centrifuged for 5 minutes at 14,500 x g to pellet the precipitate. The supernatant was then transferred to a column and centrifuged for 1 minute. 600 μL of wash buffer diluted with absolute ethanol was then used to wash the column and was subsequently centrifuged for 3 minutes to dry the column. Plasmid DNA was eluted into a new microcentrifuge tube by the addition of 30 μL of elution buffer (10 mM Tris, pH 8.5) and centrifugation at 14,500 x g for 2 minutes.

2.2.2 Plasmid Isolation from *S. aureus*

Plasmid DNA was isolated from *S. aureus* using the same protocol for *E. coli* with the addition of one step. After the pellet was resuspended in Solution I, 50 μg/mL lysostaphin was added. Cells were then incubated at 37°C for 30 minutes to allow lysis prior to the addition of Solution II.

2.2.3 Chromosomal Isolation from *S. aureus*

Chromosomal DNA from *S. aureus* was prepared using the GenElute™ Bacterial Genomic DNA Kit (Sigma) following the manufacturer's instructions. Briefly, 1.5 mL of *S. aureus* at stationary phase was pelleted via centrifugation and resuspended in 200 μL of 2.1 x 10^6 unit/mL solution of lysozyme supplemented with 50 μg lysostaphin. Cells were then incubated at 37°C for 30 minutes. 20 μL proteinase K and 200 μL Lysis Solution C was then added and was subsequently vortexed and incubated at 50°C for 10 minutes. A GenElute Miniprep Binding Column was prepared with the addition of 500 μL Column Preparation Solution and was then centrifuged at 13,000 x g. The

lysate was then prepared for binding by the addition of 200 μL absolute ethanol, vortexed for 10 seconds, and applied to the Binding Column. The column was then centrifuged at 5,000 x g. 500 μL Wash Solution I was then added to the column and centrifuged at 5,000 x g. The column was then loaded with Wash Solution Concentrate (containing 70% ethanol) and centrifuged for 3 minutes at 13,000 x g. Genomic DNA was eluted into a new microcentrifuge tube by the addition of 100 μL of elution solution to the column and subsequent centrifugation at 5,000 x g for 1 minute.

2.2.4 Restriction Enzyme Digest

All restriction enzymes used in this study were purchased from New England Biolabs (NEB). Digestions occurred in 25 μL volumes and were incubated at 37°C for 2-4 hours. Digested DNA was cleaned using GenepHlow™ Gel/PCR Kit (Geneaid) following manufacturer's instructions. Briefly, 125 μL of Gel/PCR Buffer was added to each digestion reaction. The sample was then added to a DFH Column and centrifuged at 14,500 x g for 1 minute. 600 μL of wash buffer diluted with absolute ethanol was then used to wash the column and was subsequently centrifuged for 3 minutes to dry the column. DNA was eluted into a new microcentrifuge tube by the addition of 30 μL of elution buffer (10 mM Tris, pH 8.5) and centrifugation at 14,500 x g for 2 minutes.

2.2.5 DNA Ligations

DNA ligations were performed with T4 DNA ligase purchased from NEB. DNA fragments were ligated in 25 μL reaction volumes and incubated at room temperature overnight. The 25 μL reaction was composed of 2.5 μL 10 x T4 DNA ligase reaction buffer, 1 μL T4 DNA ligase (4 x 10^5 units/mL), and a 3:1 molar ratio of insert to vector.

2.2.6 Agarose Gel Electrophoresis

Agarose gel electrophoresis was used for the separation and visualization of DNA fragments. Agarose gels (0.8% w/v) were prepared using a 1 × TAE buffer (40 mM Tris acetate, 1 mM EDTA) supplemented with 1.5 μg/mL ethidium bromide to allow visualization. To run gels, DNA samples (typically 5 μL) were mixed with loading buffer and loaded into wells in the gel. Electrophoresis was carried out utilizing a BioRad PowerPac 300 at 110 V for 30-40 minutes. A 1 kb ladder (NEB)

was utilized to determine DNA fragment size. DNA fragments were visualized using a Syngene G-Box.

2.2.7 DNA Isolation from Agarose Gels

To isolate specific DNA fragments from restriction enzyme digest, fragments were visualized with UV light and excised from agarose gel using razor blades. DNA fragments were then cleaned using GenepHlow^{TM} Gel/PCR Kit following manufacturer's instructions. Briefly, gel slices were transferred into a microcentrifuge tube and 500 μL of Gel/PCR Buffer was added. Samples were then incubated at 55-60°C until gel was completely dissolved. The mixture was then added to a DFH column and centrifuged for 1 minute at 14,000 x g. Protocol continues as described previously.

2.2.8 Polymerase Chain Reaction (PCR)

Oligonucleotides used in this study are listed in Table 2.2. PCR reactions were done in 50 μL volumes following protocols outlined by GenScript. A 50 μL reaction was composed of 5 μL x Taq buffer containing Mg^{2+}, 1 μL, dNTP, 1 μL forward primer (100 μM), 1 μL reverse primer (100 μM), 1 μL DNA template (5-100 ng/μL), 40.5 μL sterile Milli-Q water, and 0.5 μL Taq polymerase (5 units/μL). PCRs were carried out utilizing a PTC-100 Programmable Thermal Controller (MJ Research Inc.) optimized for specific primer annealing temperatures and DNA fragment lengths.

2.2.9 Nucleotide Sequencing

DNA sequencing was done at the London Regional Genomics facility of the Robarts Research Institute (London, ON) with samples prepared according to their specifications.

2.2.10 Computer Analyses

Analyses of sequenced DNA and primer design were done utilizing MacVector (MacVector, Inc, Cambridge, United Kingdom). Protein and DNA BLAST searches were performed utilizing the National Center for Biotechnology Information website (http://blast.ncbi.nlm.nih.gov/Blast.cgi).

Table 2.2 Oligonucleotides used in this study

Primer Name	Description
^{IRD800}OP4.1F	/5IRD800/TGTGTGTAGTTTAATATACAAAAT
^{IRD800}OP4.1R	/5IRD800/ATTTTGTATATTAAACTACACACA
^{IRD800}OP5.1F	/5IRD800/TTTAAATATACAGTGTAGATTATTG
^{IRD800}OP5.1R	/5IRD800/CAATAATCTACACTGTATATTTAAA
^{IRD800}OP5.2F	/5IRD800/TTTAAATATACAGTGTAAATTATTG
^{IRD800}OP5.2R	/5IRD800/CAATAATTTACACTGTATATTTAAA
farER^{IS} F	ATGACCGCGGACCATTTATGT
farER^{IS} R	GTACGGTGTACGAGTGCGTT
farR PAL2 F	GAAAATTTTGTATATTAAA**T**TACACACAAAGGAGAAATG
farR PAL2 R	CTCCTTTGTGTGTA**A**TTTAATATACAAAATTTTCCAATTG
farR ATG>TAG F	CAAAGGAGAAATGTAG**TA**GAAAGAGACTGATTTAC
farR ATG>TAG R	CAGTCTCTTTC**TA**CTACATTTCTCCTTTGTGTGTAGTTTAATATAC
farR C37A F	CAATCAAATTGCCGACAACGCACCTCGTACACCGTAC
farR C37A R	GTGCGTTGTCGGCAATTTGATTGACAGTAATCGTTTGG
farR C116A F	GTATTAAAAAATGTCGCCATTAAAATTATGCATAACGATATC
farR C116A R	GCATAATTTTAATGGCGACATTTTTTAATACTTTATTAAATTC
farR C116Y F	GTATTAAAAAATGTCT**AT**ATTAAAATTATGCATAACGATAT
farR C116Y R	GCATAATTTTAAT**AT**AGACATTTTTTAATACTTTATTAAATTC
fakA BAD F[a]	gtgaataatacaggcaa**gagctc**TTAGGAGGACAACTTGAAATGATTAGC
fakA BAD R[a]	aatta**gagctg**TTAATGATGATGATGATGATGTTCTACTGAAAAGAAATATTGATAAATTGGT
fakB2 BAD F[a]	cacatacctttctacatt**gagctc**GTAAAAAATAAGGGGGAAAACGACC
fakB2 BAD R[b]	ctcctcta**tctaga**TAATTATAAATTTAGTCTATAAAGGATTGAAATGG
farE PD F[c]	ggatagtgattgtagct**ggatcc**TTGATACCACTTGCTACAAATGCACCG
farE PD R[d]	gcaacaataataccaacta**gtcgac**AATTACCGCCTACTTCTGTAGATGTC

Lower case and bold nucleotides indicate the addition of 5´sequences to incorporate restriction endonuclease cut sites as follows: [a]SacI, [b]XbaI [c]BamHI, and [d]SalI. Nucleotides in bold and underlined show the locations of site-directed mutations.

2.3 Transformation Methodologies

2.3.1 Preparation of Transformation Competent *E. coli*

$CaCl_2$ competent *E. coli* DH5α or BL21 (DE3) were prepared for transformation following an established lab protocol. Briefly, stationary phase *E. coli* DH5α was inoculated into 400 mL LB to an OD_{600} of 0.01. When the culture reached mid-exponential phase (OD~0.5), it was placed on ice for 20 minutes. The culture was then pelleted at 4,000 x g at 4°C for 10 minutes, and cells were subsequently washed through resuspension with 100 mL 0.1M $CaCl_2$, 15% glycerol (v/v, and then left on ice for 30 minutes. Cells were pelleted again via centrifugation and pellet was resuspended in 4 mL 100 mL 0.1M $CaCl_2$, 15% glycerol (v/v) for aliquoting into 100 μL volumes. Competent cells were flash-frozen and placed in an -80°C freezer for storage.

2.3.2 Transformation of Competent *E. coli*

$CaCl_2$ competent *E. coli* DH5α or BL21 (DE3) were transformed with plasmid prepared via techniques described previously. 5 μL plasmid or 10 μL ligation mixture was added to an aliquot of thawed competent cells and incubated on ice for 30 minutes. Cells were then heat shocked at 42°C for 90 seconds, followed by a 2 minutes incubation on ice. 500 μL of LB was then added to the cells, which were then resuscitated for 1 hour at 37°C. Cells were then plated on LB agar containing relevant antibiotics. Plates were grown overnight and examined for single colonies the next day.

2.3.3 Preparation of Transformation Competent *S. aureus*

Electro-competent *S. aureus* (RN4220, USA300, and USA300 derivatives) were prepared for transformation using established lab protocols. Briefly, stationary phase *S. aureus* cells were inoculated into 400 mL TSB to an OD_{600} of 0.01. When the culture reached mid-exponential phase (OD~0.5), it was placed on ice for 10 minutes. The culture was then pelleted at 4,000 x g at 4°C for 10 minutes, and cells were subsequently washed through resuspension with 40 mL ice-cold 0.5 M sucrose, and then left on ice for 20 minutes. Cells were pelleted via centrifugation, resuspended in 5 mL 0.5 M sucrose and centrifuged again. The pellet was then resuspended in 4 mL 0.5 M

sucrose for aliquoting into 100 μL volumes. Competent cells were flash-frozen and placed in an -80°C freezer for storage.

2.3.4 Transformation of Competent *S. aureus*

Electro-competent *S. aureus* cells were transformed with plasmid DNA isolated from other cells. RN4220 is a restriction endonuclease deficient strain, and therefore can be transformed with plasmid DNA from *E. coli*. USA300 and USA300 derivates were transformed with plasmid DNA isolated from RN4220 or USA300 strains. 3 μL of plasmid DNA was added to an aliquot of thawed electro-competent cells and incubated on ice for 30 minutes. Cells were then transferred to a cold 2 mm electroporation cuvette (VWR) and electroporated using a BioRad Gene Pulser II set to 2.5 kV, 200 Ω, and 25 μF. Electroporated cells then received 900 μL TSB and were left to resuscitate for 1 hour at 37°C. Cells were then plated on TSA containing relevant antibiotics. Plates were grown overnight and examined for single colonies.

2.4 Mutagenesis and DNA Cloning Methods

2.4.1 Construction of pLI*farER* Derivative Plasmids

To construct pLI*farER* with various mutations, mutations were first made in pLI*farR* with the appropriate primers (Table 2.2). The complementation construct pLI*farR* was modified using the mutagenic primers *farR* PAL2-F and *farR* PAL2-R, using protocols and reagents following the QuikChange Site-Directed Mutagenesis Kit (Stratagene), to construct pLI*farR*4, harboring a single G>A nucleotide substitution within the TAGWTTA motif of PAL2. The same protocol was used to construct pLI*farR*$_{ATG>TAG}$, pLI*farR*$_{C37A}$, pLI*farR*$_{C116A}$, and pLI*farR*$_{C116Y}$ using mutagenic primers *farR* ATG>TAG F and *farR* ATG>TAG R, *farR* C37A F and *farR* C37A R, *farR* C116A F and *farR* C116A R, and *farR* C116Y F and *farR* C116Y R, respectively. The plasmids were then sent for sequencing at Robarts Research Institute (London, ON) to confirm the integrity of the insert. The *farER* locus was then reconstituted. Briefly, pLI50 with a *farE* insert that was previously constructed was digested with Kpn1 and SacII. The digestion mixture was then separated on an agarose gel and the 2.5 kb restriction fragment containing *farE* was then purified. The pLI*farR* plasmids containing the desired mutations were also cut with KpnI and SacII and

farE was then ligated into pLI*farR.* The reconstituted plasmid was then transformed into *E. coli* DH5α, and later *S. aureus* RN4220 and USA300 target strains following standard protocols.

2.4.2 Construction of Recombinant Plasmids

To construct pQE*farE*-PD recombinant plasmids, primers were designed according to the porter domains sequence of *farE.* The porter domain was amplified using primers *farE-PD* F and *farE-PD* R. The resulting PCR product was cleaned up and digested with BamHI and SalI and ligated into BamHI-SalI digested pQE30. The resulting construct was transformed into *E. coli* M15/pREP and colonies were screened on media supplemented with appropriate antibiotics. Positive colonies were confirmed by restriction digest and sequencing. To construct pBAD*fakAB2* primers *fakA* was first amplified using primers *fakA* BAD F and *fakA* BAD R. These primers were also modified to incorporate a C-terminal histidine tag. The resulting PCR product was cleaned up and digested with enzymes and ligated into pBAD33 that had been cut with the same enzymes. The resulting construct was transformed into *E. coli* DH5α and colonies were screened on media supplemented with appropriate antibiotics. Positive colonies were confirmed by restriction digest and sequencing. *fakB2* was then amplified using primers *fakB2* BAD F and *fakB2* BAD R. The resulting PCR product was digested with and ligated into pBAD*fakA* that had been digested with the same enzymes. Protocol was continued as mentioned previously.

2.5 Protein Methodologies

2.5.1 SDS-PAGE

Proteins were assessed using sodium dodecyl sulfate polyacrylamide gel electrophoresis (SDS-PAGE). Samples were prepared and resuspended in 10 μL 1 x Laemmli loading buffer (4 x buffer: 240 mM Tris-Cl pH 6.8, 8% w/v SDS, 40% glycerol v/v, 20% β-mercaptoethanol, 0.01% bromophenol blue and Milli-Q water). The entire sample and a pre-stained protein ladder (NEB) were loaded onto a 12% bis-acrylamide gel and run at 100 V for 90 minutes. The gel was then stained for 18 hours with Coomassie blue stain for visualization or transferred onto a membrane for Western blotting. Stained gels were destained with destaining solution (40% methanol, 10% acetic acid in dH_2O by volume).

2.5.2 Mass Spectrometry

Protein identification was achieved through mass spectrometry at the UWO MALDI MS Facility (London, ON). Proteins were separated by SDS-PAGE and stained with Coomassie blue as previously described. Proteins of interest were picked using an Ettan^{TM} spot picker. Samples were digested with trypsin and analysed using an AB SCIEX TOF System.

2.5.3 Expression and Purification of Recombinant Protein

Recombinant 6xHis-FarR, 6xHis-FarR7 or 6xHis-FarE-PD was purified from *E. coli* m15/pREP. Cultures were grown in 500 mL LB supplemented with 100 μg/mL ampicillin and 50 μg/ml kanamycin at 37^{o}C with shaking. When an OD_{600}~0.5 was reached, 0.1 mM IPTG was added, and the culture was grown with shaking at room temperature overnight. Cells were then collected via centrifugation at 4,000 x g for 20 minutes at 4°C and resuspended in 20 mL binding buffer (0.5 M NaCl, 20 mM sodium phosphate pH 7.4, 20 mM imidazole). Cells were then lysed using a cell disruptor (Constant Systems Ltd.) at 30 psi and then centrifuged for 20 minutes at 4°C and 11,000 RCF in a Beckman Coulter Optima L-900K ultracentrifuge to remove debris. The lysate was then filtered using a 0.45 μm Acrodisc syringe filter (Pall Laboratory) and applied onto a 1 mL His-Trap nickel affinity column (GE Healthcare) that had been equilibrated with binding buffer. Recombinant proteins were eluted over an imidazole gradient of 0.1 M to 0.5 M in 20 mM sodium phosphate pH 7.4. The fractions were subject to SDS-PAGE to determine purity. Fractions containing 6xHis-FarR and 6xHis-FarR7 were pooled and dialyzed in 0.15M NaCl 20 mM sodium phosphate pH 7.4 at 4°C. 6xHis-FarE-PD was further purified via anion exchange chromatography using a Resource Q column after being dialyzed into 20 mM Tris pH 7.4. Fractions were subject to SDS-PAGE to confirm purity and protein was pooled and dialyzed into 0.15 M NaCl and 20 mM sodium phosphate pH 7.4.

2.5.4 Western Blot

Rabbit polyclonal antisera recognizing FarR and FarE-PD were generated by ProSci Incorporated (Poway, CA, USA). For blots with FarR antisera, single colonies of *E. coli* DH5α transformed with pLI50, *pLIfarR*, pLI*farER*, and derivatives were inoculated in 3 mL LB supplemented with appropriate antibiotic and incubated for 8 hours at 37°C with shaking at 200 rpm. Cultures were then subcultured at an OD_{600} of 0.01 into 25 mL LB with antibiotics and grown overnight. Cells

were then pelleted via centrifugation at 4,000 x g for 10 minutes, and cells were washed with 1 x PBS. Cells were pelleted again and resuspended in 5 mL lysis buffer (150 mM NaCl, 5 mM EDTA pH 8.0, 50 mM Tris-HCl pH8.0, 1% v/v Triton X-100, 0.5% v/v SDS), supplemented with EDTA-free protease inhibitor and incubated at room temperature with agitation. The sample was then centrifuged at 4,000 x g for 20 minutes at 4°C and supernatant was collected. Protein concentration was determined by Bradford assay. 25 μg of protein sample was mixed with 10 μL 1 x Laemmli buffer and was boiled at 100°C for 5 minutes followed by centrifugation at 14,500 x g for 1 minute. The entire sample was subject to SDS-PAGE using a 12% bis-acrylamide gel, after which proteins were transferred to a PVDF membrane in a system submerged in transfer buffer (3.03 g Tris, 14.4 g glycine, 200 mL methanol, 800 mL dH_2O). The membrane was blocked overnight with blocking buffer (1 g skim milk powder, 20 mL 1 x PBS) at 4°C. The membrane was then incubated in 25 mL of primary antibody diluted 1000-fold in antibody dilution buffer (PBS containing 0.1% Tween20 and 2% w/v skim milk powder) and incubated at 4°C for 1 hour. The membrane was then washed 3 times with PBS-Tween. The membrane was then incubated for 1 hour at 4°C in 25 mL of 5000-fold diluted secondary antibody (IRDye800-conjugated goat anti-rabbit IgG; Jackson Immunoresearch Laboratories Inc.) diluted in antibody dilution buffer. Membranes were washed an additional 3 times with 1 x PBS-tween and were then imaged using Odyssey imager (LI-COR Biosciences)

2.6 Growth Analyses

For growth assays, inoculum cultures were supplemented with antibiotic where required, and these cultures were then inoculated into TSB that lacked antibiotics to assess growth in the presence of antimicrobial fatty acids. When supplementing media with fatty acid, a 5 mM stock was initially prepared in TSB with 1% DMSO. This stock was then diluted into flasks containing TSB at a 1:5 ratio of medium volume to flask size with 0.1% DMSO to achieve the desired concentration of fatty acid. Cultures were then inoculated to an initial OD_{600} of 0.01. Samples were withdrawn at hourly intervals for the determination of the OD_{600}. All cultures were grown in triplicate or as specified in individual figure legends.

2.7 EMSA

IRDye800-labeled single-stranded probes were purchased from IDT (Table 2.2). Complementary oligonucleotides were annealed at 100 μM each in 10 mM Tris pH 8.0, 0.1 mM EDTA, incubated at 95ºC for 5 minutes and allowed to cool at room temperature for 45 minutes. These probes were then used in EMSA reactions in a total 25 μL consisting of 5 μL EMSA buffer (20% glycerol, 30 mM Tris-HCl pH 8.0, 1 mM $MnCl_2$, 120 mM KCl, 1 mM $MgCl_2$, 16 mM DTT), 240 μg/mL BSA, 15.2 μg/mL poly[d(I-C)], 5 pmol of probe, and up to 2 μM recombinant 6xHis-FarR or 6xHis-FarR7. The reaction was incubated at room temperature for 60 minutes, after which they were run on a 6% TBE-acrylamide gel at 120 V for 45 minutes and imaged using Odyssey imager (LI-COR Biosciences). For EMSA conducted using the 339 bp *farER* intergenic segment, PCR products were amplified as described above, using 5 pmol of PCR product, and after electrophoresis, the EMSA gel was stained with 3 μg/mL prior to imaging using Syngene G-Box.

3 Results

3.1 Evaluation of Nucleotide Substitutions in FarR DNA Operator sites

3.1.1 Mutations in O_{farR} and O_{PAL1} relieve autorepression but do not cause increase in resistance to linoleic acid

Our lab has previously identified three operator sites for FarR within the intergenic segment (Fig. 1.2). These include O_{farR} which overlaps with P_{farR}, O_{PAL1} which overlaps both PAL1 and P_{farR}, and O_{farE} which lies upstream of P_{farE}. Additionally, all three operator sites contain a common motif of TAGWTTA. The positions of both O_{farR} and O_{PAL1} are consistent with a role in auto-repression, and we have previously shown that a G>A substitution in the conserved TAGWTTA motif of O_{farR}, alleviates autorepression of *farR* (82). To support this finding, we wanted to determine whether this mutation in O_{farR}, hereafter referred to as pLI*farER*1 and mutations in O_{PAL1} cause a decrease in the binding of these operator sites (Fig 3.1A). Mutations were made in the inverted repeats of O_{PAL1}, hereafter referred to as pLI*farER*2 and EMSA were done with the entire intergenic segment containing these mutations (Fig 3.1B). EMSA done with WT FarR and the native IS displays three discrete mobility shifts designated S1, S2, and S3, consistent with there being three operator sites O_{farR}, O_{PAL1}, and O_{farE}. When EMSA was conducted with the *farER*1-IS, the S2 shift was eliminated indicating that this corresponds to FarR binding to the O_{farR} site. However, when EMSA was conducted with the *farER*2^{IS}, both the S1 and S2 shifts were eliminated. This suggests that FarR binds preferentially to O_{PAL1} and the secondarily to O_{farR}, since both the S1 and S2 shifts were eliminated with nucleotide substitutions in the O_{PAL1} site of the *farER*2 construct. By default, these observations imply that the S3 supershift is due to FarR binding to O_{farE}, since this site is not affected in the *farER*2 construct. In support of this conclusion, EMSA with the *farER*3^{IS} construct harboring substitutions in both O_{farR} and O_{PAL1} still yielded the S3 shift.

Western blots for the detection of FarR were then performed using lysates of *E. coli* DH5α transformed with pLI*farER* derivatives, to evaluate how these substitutions affected autorepression of FarR expression (Fig 3.1C). We found that mutations made in both O_{farR} and O_{PAL1} caused an increased amount of FarR present in lysates. More FarR was detected with constructs harbouring

mutations in O_{PAL1} compared to those where only O_{farR} was affected, which is consistent with our finding that the binding of O_{farR} is dependent on O_{PAL1}. Previous experiments in our lab have also discovered FAR7, a variant strain of USA300 that demonstrates increased resistance to linoleic acid due to a H121Y substitution in FarR. This substitution causes FarR7 to not be able to bind to O_{farR}, but it is able interact well with O_{farE} as shown by EMSA (Fig 3.1B). This relief of auto-repression increases the resistance to uFFA due to increased expression of *farE*, even without the addition of uFFA. We therefore hypothesized that the abrogation of binding to O_{farR} and O_{PAL1} should increase resistance to linoleic acid due to the increased production of FarR. However, we found that mutations in both O_{farR} and O_{PAL1} decrease resistance to uFFA, even though these mutations cause strong de-repression of *farR* expression (Fig 3.1D). Therefore, constitutive expression of wild type FarR was unable to promote increased resistance to antimicrobial uFFA, which is uniquely associated with the H121Y variant in FarR7.

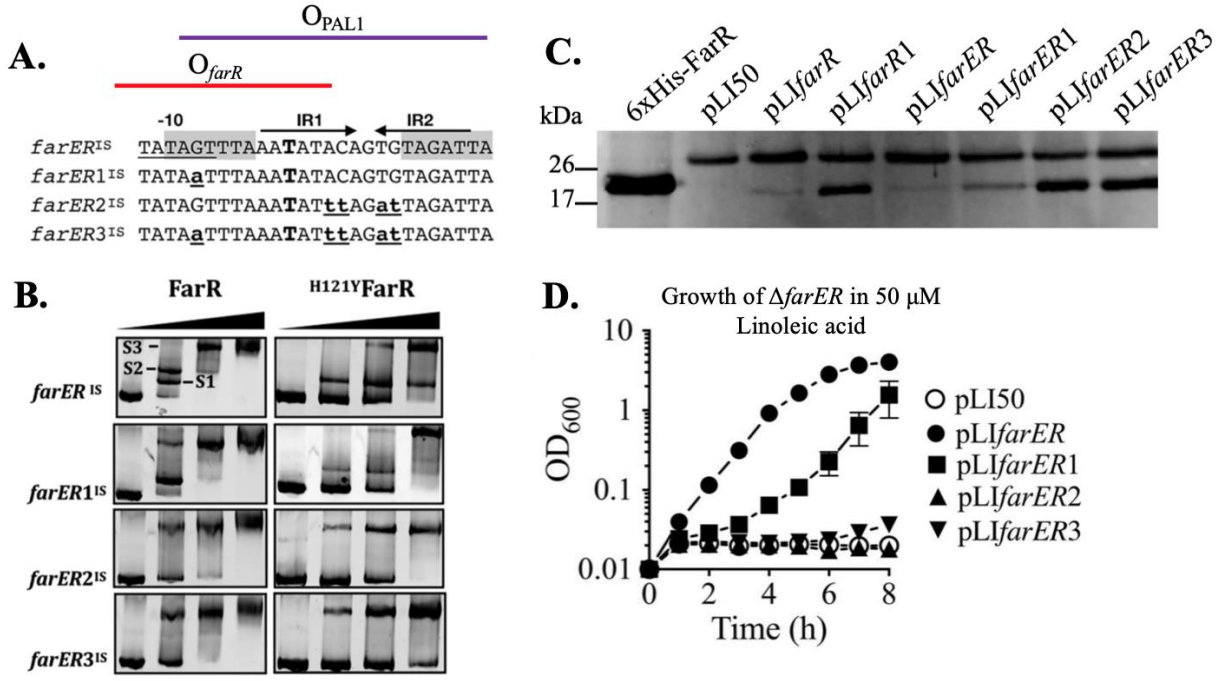

Figure 3.1 Mutations in O_{farR} and O_{PAL1} relieve autorepression but do not cause an increase in resistance to linoleic acid. (A) Nucleotide sequence showing the variable segments of the 144bp *farER*^{IS}, *farER*1^{IS}, *farER*2^{IS}, and *farER*3^{IS} probes containing nucleotide substitutions in O_{farR} (pLI*farER*1, PAL1 (pLI*farER*2), or O_{farR} and PAL1 (pLI*farER*3). The labeled features above *farER*^{IS} are as detailed for Fig. 2A. The larger bold type "T" in IR1 indicates the +1 transcription start site of *farR*. Lowercase underlined nucleotides indicate nucleotide substitutions that differentiate each probe. **(B)** EMSA was conducted with 5 pM probe and 0, 0.5, 1, or 2 μM FarR or ^{H121Y}FarR, as indicated. The first lane of each panel represents electrophoresis of the *farER*^{IS} probe without added protein (i.e., 0 μM FarR). In the upper-left panel, the protein-DNA complexes S1, S2, and S3 are labeled. Protein-DNA complexes were directly imaged by ethidium bromide staining. **(C)** Western blot of gel loaded with 25 ng of purified 6xHis-FarR or 25 μg of cell lysate protein from *E. coli* DH5α transformed with pLI50 vehicle, pLI*farR*, or pLI*farER* and derivatives. **(D)** Growth of USA300Δ*farER* complemented with pLI50 vehicle or pLI*farER* and derivatives in TSB plus 50 μM linoleic acid. Each data point represents the mean and standard deviation of the results from triplicate cultures.

3.1.2 Mutations in PAL2 cause a loss of resistance to linoleic acid

We have shown that mutations in the common TAGWTTA motif of both O_{farR} and mutations in PAL1 of O_{PAL1} cause a loss of autorepression of *farR* (Fig 3.1B) (82). However, the role of the TAGWTTA within the potentially activating O_{farE} operator site has not been elucidated. O_{farE} lies upstream of P_{farE} and contains PAL2 which is composed of IR1 and IR2a (Fig. 1.2). Additionally, the common TAGWTTA motif lies within. Since a G>A nucleotide substitution in the TAGWTTA motif of O_{farR} abrogated FarR binding (Fig. 3.1B), we hypothesized that a G>A substitution in the TAGWTTA motif of PAL2, would likewise abrogate binding to this potentially activating site, and subsequently cause a loss in resistance to linoleic acid. This G>A mutation in the TAGWTTA motif of O_{farE} was introduced into pLI*farER* constituting the pLI*farER*4 construct, which was subsequently transformed into USA300Δ*farER* for growth analyses (Fig 3.2A). Accordingly, we found that the elimination of the conserved binding sequence does cause a loss of resistance to linoleic acid. EMSA were then done using probes of the native $farER^{IS}$, and the $farER4^{IS}$ harbouring the G>A substitution in the TAGWTTA motif of PAL2 (Fig 3.2B). Surprisingly, the mobility shift pattern was not altered, as S3 was still visible when PAL2 was mutated, indicating that FarR can still bind to O_{farE} even when the TAGWTTA motif is altered. However, even though FarR can still bind to O_{farE} when the TAGWTTA motif is altered, there is still a loss of resistance to linoleic acid.

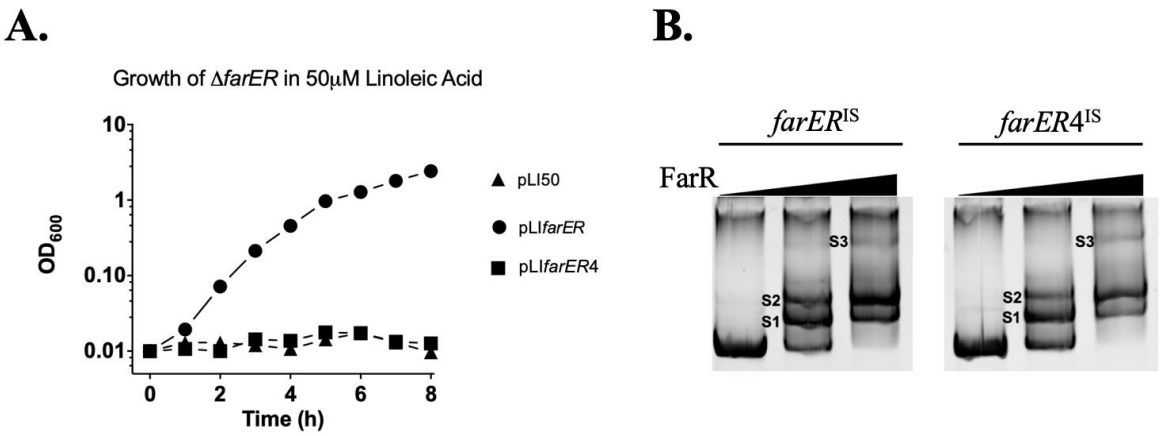

Figure 3.2 Mutations in PAL2 cause a loss in resistance to linoleic acid. (A) Growth of USA300 Δ*farER* complemented with pLI50 vehicle or pLI*farER* and derivatives in TSB plus 50 µM linoleic acid. Each data point represents the mean and standard deviation of the results from triplicate cultures. **(B)** EMSA was conducted with 5 pM of WT *farER*^{IS} or PAL2$_{G>A}$ *farER*4^{IS} probe and 0, 0.5, 1, or 2 µM FarR. The first lane of each panel represents electrophoresis of the *farER*^{IS} probe without added protein (i.e., 0 µM FarR). In the upper-left panel, the protein-DNA complexes S1, S2, and S3 are labeled. Protein-DNA complexes were directly imaged by ethidium bromide staining.

3.1.3 Significance of the TAGWTTA motif is context dependent

When EMSA were done with the entire intergenic segment, FarR was able to bind to both O_{PAL1} and O_{farE}, as shown by shifts S1 and S3, respectively (Fig. 3.1 B). However, when the O_{farE} site was altered and EMSA was conducted with the resulting *farER*4^{IS}, the S3 shift remained evident. We therefore conducted additional EMSA to assess the specificity of FarR binding to a probe containing the minimal PAL1 and PAL2 segments, both of which contain the common TAGWTTA motif. Additionally, as we have previously shown that a G>A substitution in the TAGWTTA motif of O_{farR} abrogated binding, we wanted to determine if a similar G>A mutation in the PAL1 TAGWTTA would do the same (82). EMSA were done with minimal PAL1 or PAL2 probes that were both extended by 4 nucleotides at each end (Fig 3.3A). FarR was able to bind to a minimal PAL1 probe, as well as to a minimal PAL1 probe with a G>A in the TAGWTTA, albeit to a lesser extent (Fig 3.3B). However, FarR was unable to interact with a minimal PAL2 probe compared to the S3 supershift of the entire intergenic segment probe (Fig 3.1B). It is important to note that PAL1 and PAL2 are composed of similar or identical inverted repeat half sites (IR1 and IR2/2a), with their positions in PAL2 being juxtaposed relative to PAL1. Therefore, although both PAL1 and PAL2 contain the common TAGWTTA motif, FarR exhibits differential binding to these sites, recognizing a probe containing the minimal PAL1 segment, but not PAL2. From these observations, we are not able to conclude that the S3 shift observed in EMSA is due to specific binding of FarR to PAL2.

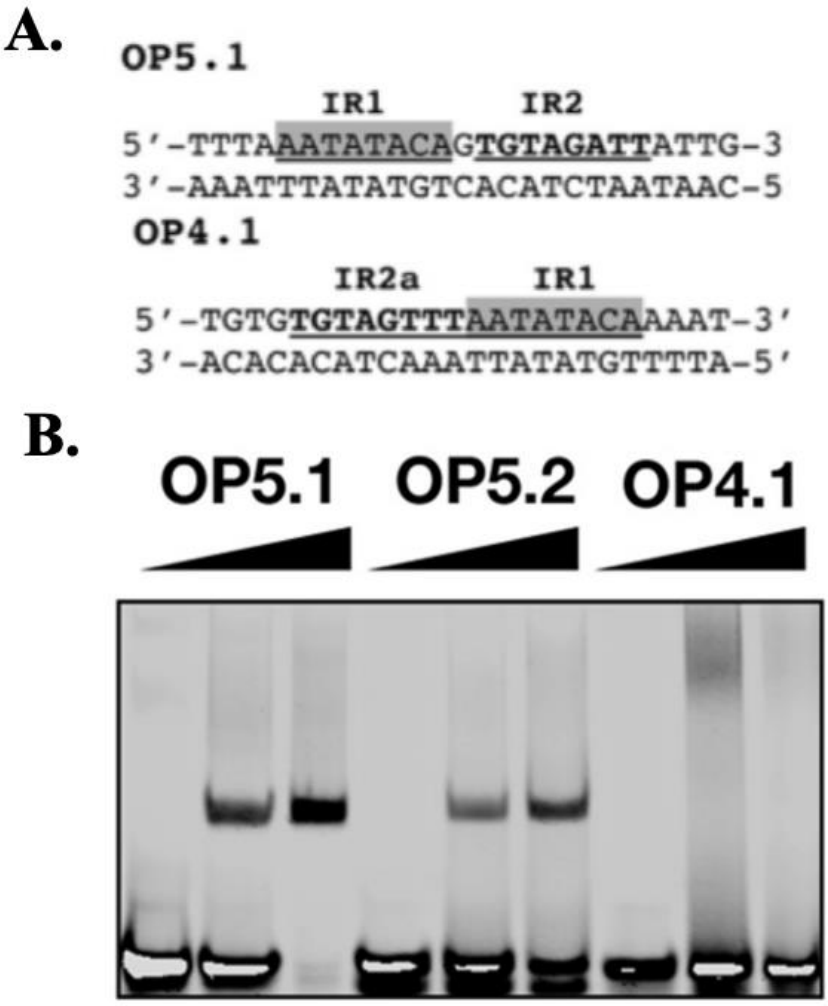

Figure 3.3 Significance of the TAGWTTA motif is context dependent. **(A)** Composition of PAL1 (OP5.1) and PAL2 (OP4.1) probes. Nucleotides comprising the inverted repeat IR1, IR2, and IR2a components of PAL1 and PAL2 are underlined. The IR1 half-site is shaded, while the IR2 and IR2a half-sites are in bold type. Probe OP5.2 is identical to OP5.1, with the exception of a G>A substitution in the TAGATTA motif that overlaps IR2. The top strand contains a 5' IRDye 800 addition. **(B)** EMSA with 0, 0.2, or 0.5 µM FarR mixed with 5 pM OP5.1, OP5.2, or OP4.1, as indicated.

3.2 Investigation into *farR* leader mRNA

3.2.1 Resistance to linoleic acid is not mediated by *farR* leader mRNA itself

There are examples of some TFRs that utilize RNA-mediated post-transcriptional mechanisms to regulate the target gene. In *Mycobacterium smegmatis* AmtR is a global regulator of nitrogen metabolism. When nitrogen is abundant, cis-encoded small RNAs (sRNA) complementary to *amtR* mRNA blocks transcription (95). LuxR, a TFR in *Vibrio harveyi* is also regulated by sRNAs by complementary base pairing to the 5′UTR (96). Additionally, sRNAs often target the 5′UTR of mRNA. The *farR* mRNA has a 105bp long 5′UTR that may be target for sRNA, or other mechanisms of RNA mediated regulation, such as riboswitches. Moreover, the 5′ ends of *farE* and *farR* mRNA overlap through 21nt that could have a negative impact on the stability or translation and could promote degradation through dsRNA ribonucleases. To determine if the 5′UTR of *farR* was responsible for the activation of *farE* itself in the absence of FarR protein, the start codon of *farR* was mutated to a stop codon. FarR was only slightly detected in *E. coli* lysates harbouring pLI*farR*$_{ATG>TAG}$, indicating that this mutation did appear to stop the majority of *farR* translation (Fig 3.4A). USA300Δ*farER* complemented with pLI*farER*$_{ATG>TAG}$ was unable to grow in 50 µM linoleic acid indicating that the *farR* 5′UTR mRNA is not in itself sufficient to promote resistance to linoleic acid and confirming that functional FarR protein is required for expression of FarE (Fig 3.4B).

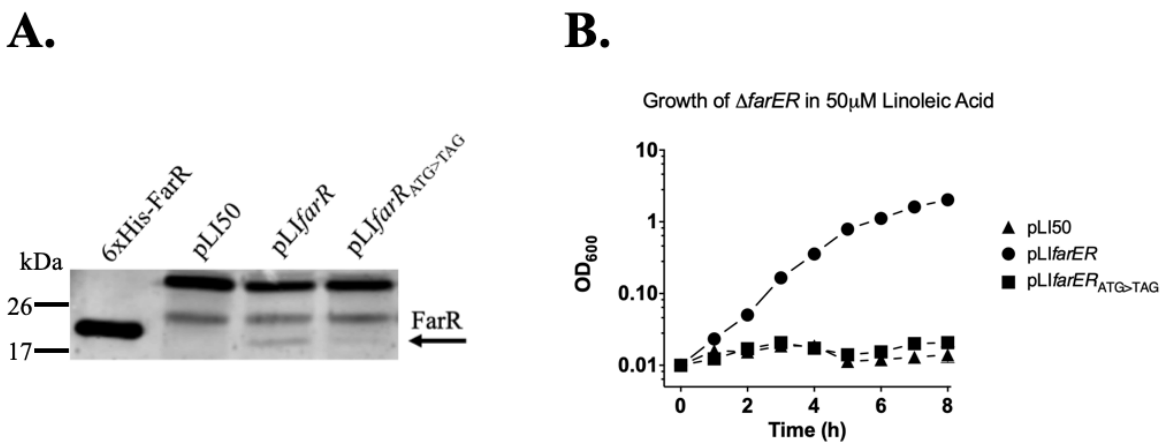

Figure 3.4 Resistance to fatty acid is not mediated by *farR* leader mRNA itself. (A) Western blot of gel loaded with 25 ng of purified 6xHis-FarR or 25 µg of cell lysate protein from *E. coli* DH5α transformed with pLI50 vehicle, pLI*farR*, and pLI*farR*$_{ATG>TAG}$. **(B)** Growth of USA300 Δ*farER* complemented with pLI50 vehicle or pLI*farER* and derivatives in TSB plus 50 µM linoleic acid. Each data point represents the mean and standard deviation of the results from triplicate cultures.

3.3 Role of cysteine residues in FarR function

3.3.1 Mutation of cysteine residues result in loss of resistance to linoleic acid

Other regulators in *S. aureus*, like SarA, use the oxidation of cysteine residues to modulate DNA binding and regulation. SarA regulates many genes both directly and indirectly including hemolysins, fibronectin and fibrinogen binding proteins, enterotoxins as well as *trxB*. TrxB maintains TrxA, thioredoxin, in a reduced form allowing it to maintain the intracellular thiol-disulfide balance. The oxidation of Cys9 in SarA has been shown to reduce the binding of SarA to the promoter of *txrB* (97). Arachidonic acid (20:4), a polyunsaturated free fatty acid, is released from macrophages during the oxidative burst and has been shown to kill *S. aureus* through lipid peroxidation, creating an oxidative environment in the cell (48). This is of importance as our lab has previously shown arachidonic acid as the strongest known inducer of *farE* expression (56). Therefore, we wondered whether cysteine residues were important in FarR function.

FarR contains two cysteine residues. Cys37 lies within the N-terminal DNA binding domain and is conserved in all FarR proteins in *S. aureus.* Cys116 lies within the C-terminal ligand binding domain and is not as conserved as Cys37 (Fig 3.5A). Site directed mutagenesis was done, using pLI*farER* as a template, to mutate either cysteines to an alanine residue. The mutated pLI*farER* plasmids were then used to complement USA300Δ*farER* and susceptibility to linoleic acid was determined (Fig 3.5B). We found that the mutation of either cysteine was sufficient to eliminate resistance to linoleic acid. As previously mentioned, mutations in O_{farR} and O_{PAL1} relieve autorepression and cause an increased amount of FarR present in lysate. However, this increase in FarR levels causes a decrease in the resistance to linoleic acid. As Cys37 lies within the DNA binding domain of FarR, we wondered whether Cys37 could be involved in DNA binding and autorepression. If Cys37 is involved in the autorepression of *farR*, the introduction of an alanine residue in this position could relieve autorepression, leading to increased levels of FarR and could explaining the decrease in resistance to linoleic acid. Western blots for detection of FarR were done in *E. coli* lysates transformed with pLI*farR* C37A or C116A. These Western blots revealed a decreased amount of ^{C116A}FarR relative to WT FarR (Fig 3.5C). Interestingly, there was a complete absence of ^{C37A}FarR, indicating that this mutation may cause super-repression of *farR*.

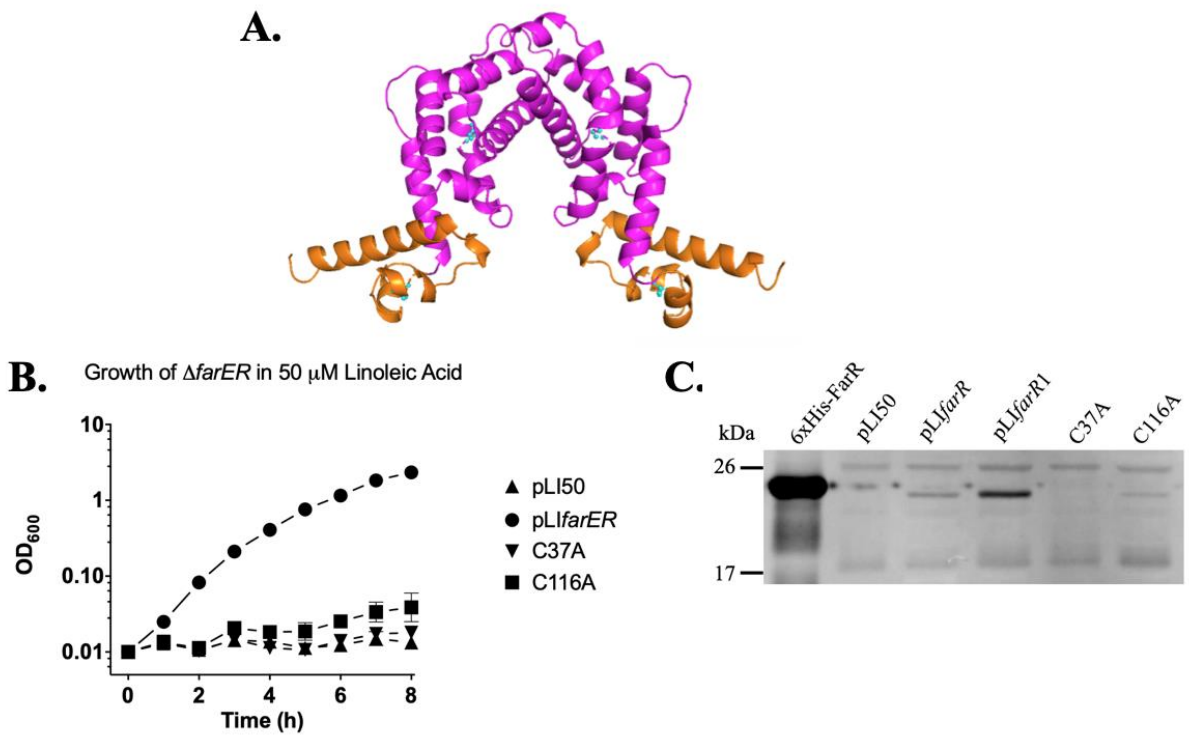

Figure 3.5 Cysteine residues are necessary for FarR function. (A) Structure of FarR homodimer. Orange represents N-terminal DNA binding domain. Pink represents ligand binding domain. Both cysteine-37 and cysteine-116 are labeled in blue. **(B)** Western blot of gel loaded with 25 ng of purified 6xHis-FarR or 25 µg of cell lysate protein from E. coli DH5α transformed with pLI50 vehicle, pLI*farR*, and pLI*farR* derivatives. **(C)** Growth of USA300 Δ*farER* complemented with pLI50 vehicle or pLI*farER* and derivatives in TSB plus 50 µM linoleic acid. Each data point represents the mean and standard deviation of the results from triplicate cultures.

3.4 Assessing influence of amino acid variation in FarR sequence

3.4.1 C116Y substitution causes increase in production of FarR compared to C116A

As mentioned previously, FarR7 (^{H121Y}FarR) exhibits increased expression of both *farR* and *farE,* even in non-inducing conditions and therefore, an increased resistance to linoleic acid. Additionally, a recent study found that a C116R substitution in FarR causes constitutive activation of *farE* (98). C116 and H121 are in close proximity and both lie within the same alpha helix in the ligand binding domain of FarR. Therefore, we wondered whether a C116Y substitution would cause a similar phenotype to both the H121Y and C116R mutants in which *farE* is constitutively expressed. Western blots for detection of FarR in *E. coli* lysates transformed with pLI*farR* H121Y or pLI*farR* C116Ywere done and we found that levels of ^{C116Y}FarR were increased compared to that of ^{C116A}FarR (Fig 3.6). However, levels of ^{C116Y}FarR was not as abundant as ^{H121Y}FarR and was more comparable to that of WT FarR. It remains to be determined if this C116Y mutant causes an increase in resistance to linoleic acid.

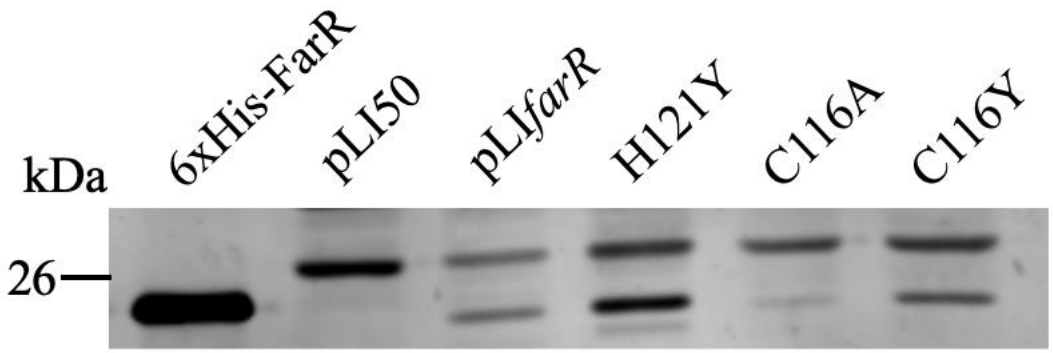

Figure 3.6 Role of tyrosine in the ligand-binding domain of FarR. Western blot for detection of FarR. Gel was loaded with 25 ng of purified 6xHis-FarR or 25 µg of cell lysate protein from *E. coli* DH5α transformed with pLI50 vehicle, pLI*farR*, and pLI*farR* derivatives.

3.4.2 *S. aureus* ^{C116Y}FarR clinical isolates have variable resistance to linoleic acid

We have determined that a C116Y substitution in FarR increases the abundance of FarR found in *E. coli* lysates compared to that of a C116A substitution, albeit not to the same extent as a H121Y substitution. It has been previously established that this H121Y substitution in FarR causes constitutive expression of *farE,* leading to resistance to linoleic acid. In contrast, USA300Δ*farER* complemented with pLI*farER*$_{C116A}$ is unable to grow in 50 μM linoleic acid. As it appears that increased abundance of ^{H121Y}FarR protein leads to increased resistance, we speculated that the C116Y substitution may likewise promote increased resistance to linoleic acid. When BLAST analysis was conducted to compare the FarR protein of *S. aureus* USA300 to all other *S. aureus* genome sequences, over 3000 strains have a cysteine at position 116. However, 11 strains have a tyrosine at position 116, all of which are MRSA (Table 3.1). Some of these strains were grown in TSB supplemented with 50 μM linoleic acid to determine whether they were resistant to fatty acid, similar to the FAR7 strain. Out of the 6 that we were able to test, 2 clinical isolates appear to be more resistant to linoleic acid (M0330 and M1545) (Fig 3.7 A and B). M0390 appears to be somewhat resistant to linoleic acid, but not to the extent that M330 and M1545 are. Further characterization of these clinical isolates needs to be done, including sequencing to confirm the C116Y substitution, as well as to determine if there are additional mutations that may account for the increased resistance to linoleic acid as seen here.

Table 3.1 Clinical isolates of *S. aureus* ^{C116Y}FarR

Strain	Location of Isolation
M0049	Sputum
M0182	Unknown
M0194	Sputum
M0330	Unknown
M0374	Blood
M0377	Sputum from endotrachea
M0390	Sputum
M0398	Wounds
M0402	Nares
M0423	Bronchial Washings
M01545	Nares

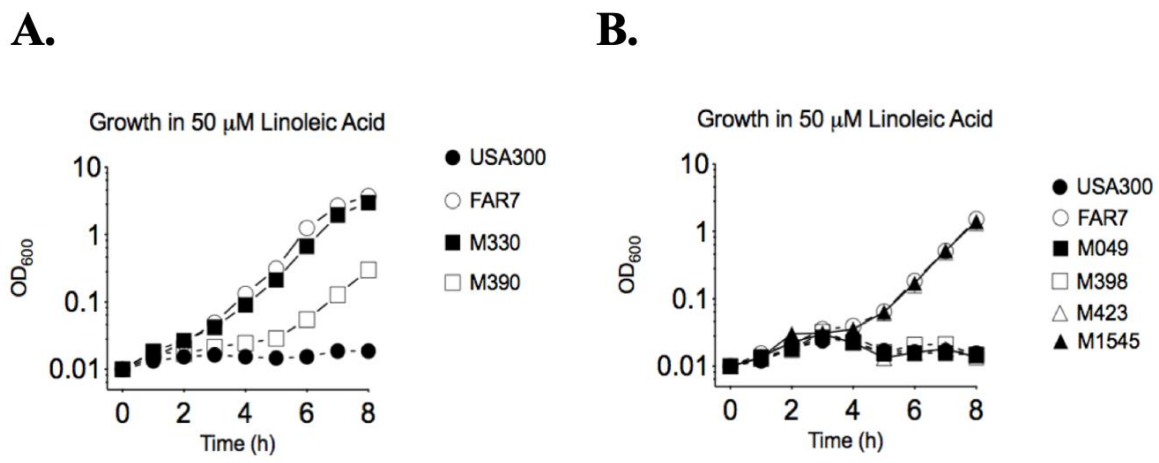

Figure 3.7 Growth of *S. aureus* ^{C116Y}FarR clinical isolates in linoleic acid. (A)(B) Growth of USA300, FAR7 and indicated clinical isolates in TSB plus 50 μM linoleic acid. Each data point represents the mean and standard deviation of the results from triplicate cultures.

3.5 Assessing the Role of acyl-phosphates for the activation of *farE* expression

3.5.1 Co-expressing *fakAB*2 and *farER* in *Escherichia coli*

One tenet of TFR function is the ability of a ligand to modulate the DNA binding affinity of the TFR, enabling it to repress or activate transcription of the regulated gene. However, the physiological ligand of FarR remains unknown. A previous study in our lab has observed that in USA300ΔfakA, *farE* is unable to be fully induced (82). As mentioned previously, FakA is a kinase that catalyzes the first step in the incorporation of exogenous fatty acids into membrane phospholipids (58). Therefore, we hypothesize that the identity of the ligand may be an acyl-phosphate. To test this hypothesis, we co-expressed *fakA* and *fakB2* in *E. coli* under the expression of the arabinose inducible pBAD33 promoter. *fakA* was cloned under control of the pBAD promoter with *fakB2* cloned in directly after. FakB2 was chosen over FakB1 as FakB2 preferentially binds unsaturated fatty acids. Concurrently, *E. coli* was transformed with pLI*farER* containing *farE* and *farR* expressed from their native promoters. If our hypothesis is correct, induction of *fakAB* with arabinose will lead to production of an acyl-phosphate, which in turn will be bound by FarR, and lead to the induction of *farE* (Fig. 3.8A). We chose to approach this experiment in a heterologous host, as if successful, it would elucidate the minimal combination of genes necessary to induce *farE* expression.

First, *E. coli* DH5α transformed with pBAD*fakAB*2 was induced with arabinose to confirm the production of FakA and FakB2(Fig 3.8B). The identities of both proteins were confirmed via mass spectrometry analysis. To determine whether the presence of FakAB2 and phosphorylated fatty acids increase the expression of FarR, Western blots for detection of FarR were done on *E. coli* lysates grown in LB with the addition of 50 μM LA and 0.1% L-arabinose when stated to induce *fakAB2* expression. *E. coli* does produce palmitoleic and oleic acid as endogenous fatty acids, however, previous work has shown that these uFFA do not induce *farE* expression as strongly as linoleic or arachidonic acid (56,99); therefore linoleic acid was added to the cultures. Lysates of DH5α harbouring pLI*farR*1, in which *farR* is de-repressed, was used as a positive control. There appears to be a similar amount of FarR present when co-expressed with *fakAB2* compared to pLI*farER* but not compared to lysates harbouring pLI*farR*1, in which FarR is de-repressed (Fig

3.8C). This indicates that, if acyl-phosphates were generated, their presence does not directly influence the abundance of FarR in the lysate. However, it is unknown whether the presence of both FakAB2 and phosphorylated fatty acids influence the amount of *farE* present in lysates.

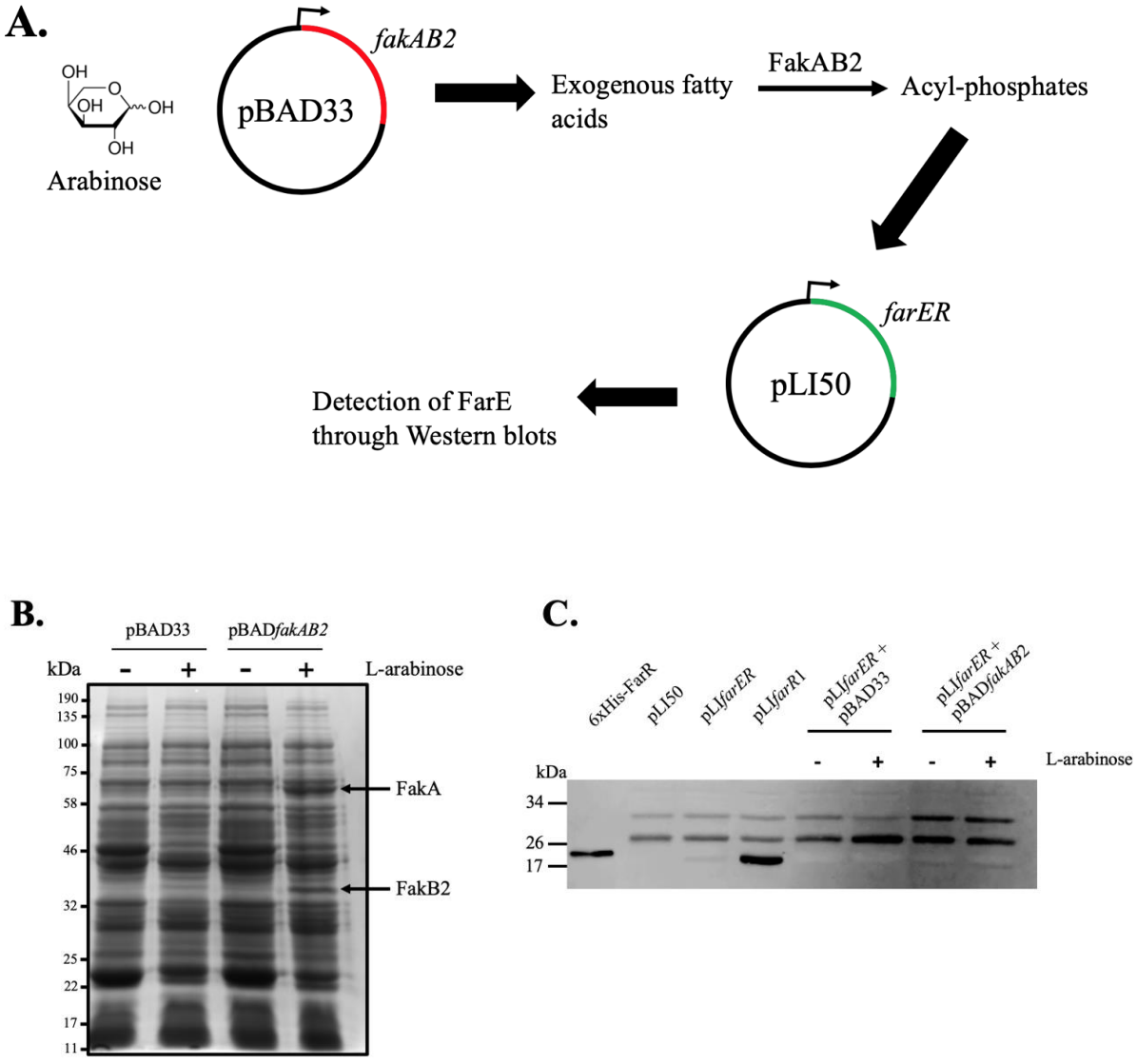

Figure 3.8 Co-expression of *fakAB2* and *farER* in *E. coli* DH5α. (A) Schematic of experimental design. 1% L-arabinose and 50 μM linoleic acid were added to *E. coli* cultures at OD_{600} ~ 0.5. Cells were grown for an additional 2 hours before being lysed for Western blots. **(B)** SDS-PAGE of *E. coli* DH5α lysate harbouring pBAD*fakAB2* or empty vector. Cultures were induced at mid-exponential phase with 0.1% L-arabinose and grown for 2 hours. **(C)** Western blot for detection of FarR. Gel was loaded with 5 μg of purified 6His-FarR or 25 μg of cell lysate protein from DH5α transformed with indicated plasmids.

3.5.2 Production of anti-FarE-PD antibodies

In order to detect the presence of FarE in *E. coli* co-expressing both FakAB2 and FarER, we set out to generate anti-FarE antibodies. Previous attempts to generate anti-FarE antibodies against the C-terminal coiled coil domain of FarE were unsuccessful, possible due to the tendency of the recombinant protein to precipitate. Porter domains of RND-family efflux pumps, which are responsible for substrate recognition and binding, are soluble. Therefore, we chose to purify a porter domain of FarE (FarE-PD) for antibody production (100). *farE-PD* was cloned into pQE30 and purified via metal affinity chromatography and was further purified using anion exchange chromatography (Fig 3.9A and B). However, it was difficult to purify large amounts of FarE-PD, and the amount that was purified degraded very quickly, degrading after only one freeze-thaw cycle (Fig 3.9C). Nonetheless, what was purified was sent for polyclonal antibody production in New Zealand white rabbits. The anti-FarE-PD antibodies were able to recognize purified FarE-PD on a Western blot (Fig 3.9D). However, we were unable to identify whole FarE protein from either *E. coli* harbouring *farE* on an inducible plasmid, or USA300 grown in the presence of linoleic acid.

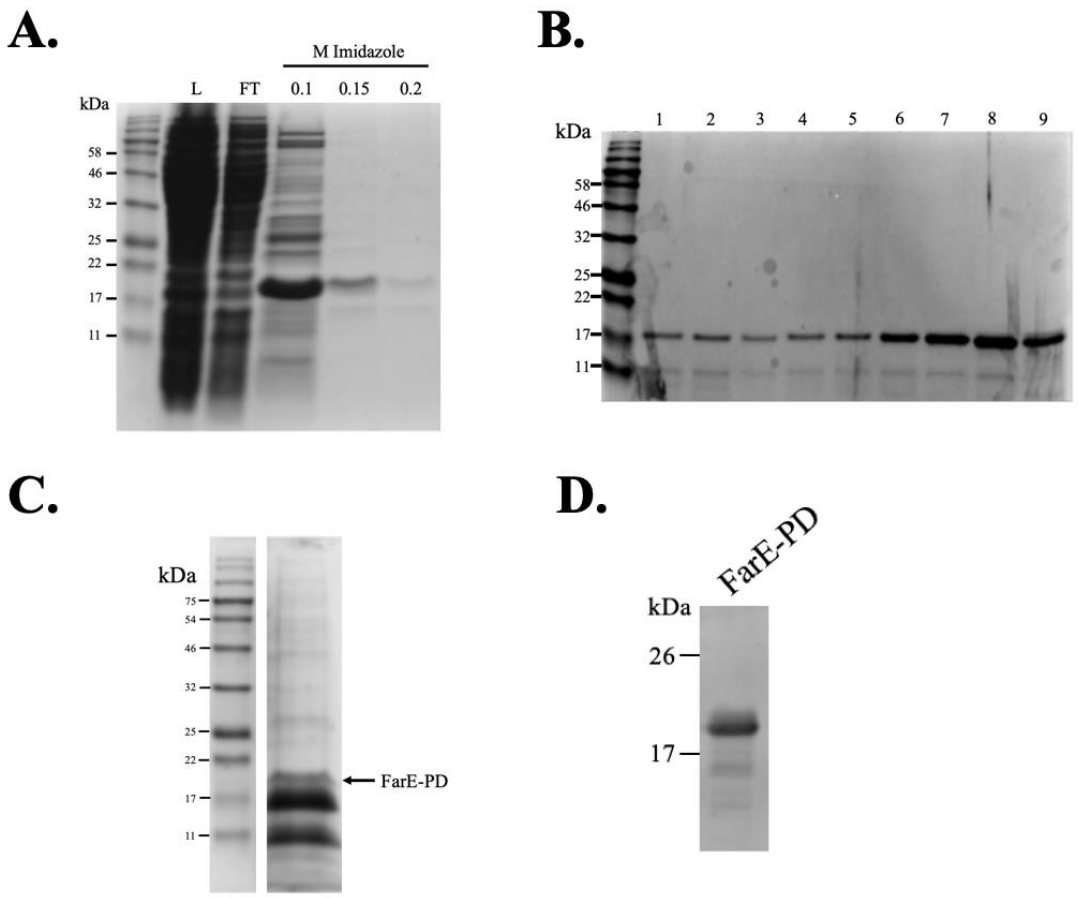

Figure 3.9 Production of anti-FarE-PD antibodies. (A) Cell lysate was applied onto a 1 mL His-Trap nickel affinity column that was equilibrated with binding buffer (20 mM sodium phosphate, 0.5 M NaCl, 20 mM imidazole, pH 7.4). After washing with binding buffer, bound His-tagged protein was eluted over a step-wise imidazole gradient (0.1-0.5 M) in 20 mM sodium phosphate. Column fractions were assessed by SDS-polyacrylamide gel electrophoresis to check for purity. L is the total cell lysate, and FT is the washed flow through fraction. Purified FarE-PD protein band is at ~ 19 kDa **(B)** 0.1M fraction from A was applied onto a Resource Q ion exchange column. Sample was eluted with a gradient buffer of 0.5M NaCl, 20mM Tris pH 8.0 **(C)** SDS-PAGE of purified FarE-PD after fractions A1-A9 were pooled, dialyzed, concentrated, then frozen and thawed. Arrow indicates where samples were taken for mass spectrometry analysis. **(D)** Western blot for detection of FarE-PD. Gel was loaded with *E. coli* pQE*farE-PD* lysates induced with IPTG.

4 Discussion

USA300 has emerged as the leading cause of *S. aureus* infections and a cause of life-threatening infections irrespective of hospital or community setting due in part to its enhanced ability to persist on human skin. In order to effectively colonize the skin, USA300 must overcome innate defence mechanisms, including antimicrobial unsaturated free fatty acids found in the sebum and as well as in the context of tissue abscesses where *S. aureus* is also exposed to high levels of linoleic acid (101). Our lab has identified the genes *farR* and *farE,* as a regulator and effector pair that confer resistance to unsaturated free fatty acids. *farR* encodes a TFR and is needed for the expression of *farE,* an RND-family efflux pump that promotes efflux of uFFA. However, the exact mechanism through which *farE* is regulated by *farR* is unclear and the aim of this research was to elucidate the mechanism through which *farE* expression is regulated by FarR.

FarR belongs to the family of Type I TFR due to the divergent arrangements of genes, and on this basis was expected to repress both its own expression, and the expression of the divergently transcribed *farE*. However, FarR represents an unusual TFR as it has dual roles as both and activator and repressor of *farE* expression (57, 83). FarR binds three operator sites in the *farER* intergenic segment, O_{farE}, O_{farR}, and O_{PAL1}, all of which contain a conserved TAGWTTA motif. The positions of both O_{farR} and O_{PAL1} as overlapping the promoter of *farR,* would be consistent with a role in autorepression. O_{farR} overlaps entirely with the *farR* promoter and O_{PAL1} lies slightly downstream and contains PAL1, in which the TAGWTTA motif is found (Fig 1.2). We have shown that with a loss of either this common motif in O_{farR} or with several nucleotide substitutions in O_{PAL1}, FarR is unable to bind to these operator sites (Fig 3.1B). Additionally, we have shown evidence through EMSA of cooperative binding in which FarR firsts binds to O_{PAL1} and then to O_{farR}, since the disruption of PAL1 also leads to loss of mobility shift attributed to binding of the adjacent O_{farR} (Fig 3.1B). Cooperative binding has been shown in other TFRs as well. In *Dietzia* species, regulation of alkane degradation is carried out by AlkX, which like other TFRs negatively regulates its own expression. The inverted repeat that is bound by AlkX is unusually long, being 48 bp and AlkX has been shown to bind cooperatively as a pair of dimers to two adjacent operator sites within (102). Additionally, QacR in *S. aureus* has been shown to bind cooperatively as a dimer of dimers (75). Similarly to AlkX, QacR recognizes an unusually large inverted repeat that

is 28 bp long. QacR functions as a tetramer and it has been shown that each dimer binds to each inverted repeat half-site cooperatively (77).

With the loss of binding to O_{farR} and O_{PAL1}, FarR is de-repressed as shown by Western blots (Fig 3.1C). FarR is more readily detected when O_{PAL1} is mutated, compared to the mutation of just O_{farR}, further supporting our earlier finding that the binding of O_{farR} is dependent on initial binding to O_{PAL1}. Since *farE* cannot be expressed in the absence of FarR function, we anticipated that de-repression of *farR* would lead to an increase in resistance to linoleic acid. However, this was not the case, as increasing abundance of FarR seems to decrease the resistance to linoleic acid, as was evident when the pLI*farER* and pLI*farER*1 or pLI*farER*2 constructs were tested for their ability to complement the USA300Δ*farER*. These results are inconsistent with what was observed with the FAR7 strain. FAR7 expresses a H121Y variant of FarR that leads to de-repression of *farR* combined with constitutive expression of *farE* in the absence of fatty acid, and a higher induced level of *farE* expression compared to wild type USA300 (56). These observations point to a fundamental difference in the behaviour of wild type FarR and ^{H121Y}FarR expressed by the FAR7 strain. Namely, ^{H121Y}FarR exhibited loss of binding to O_{farR}, leading to de-repression of *farR* expression and constitutive expression of *farE.* In contrast, although a nucleotide substitution in the TAGWTTA motif of O_{farR} was able to phenocopy the de-repression of *farR* observed in the FAR7 strain, it failed to phenocopy the constitutive expression of *farE* and increased resistance to linoleic acid. This can be taken as evidence to support the hypothesis that the H121Y substitution in FarR allows the protein to mimic a ligand-bound conformation, which is necessary to activate *farE* expression. Additionally, the observation that increased FarR expression does not lead to increased resistance may be explained by the abundance of FarR in relation to the amount of ligand present. Perhaps there needs to be an appropriate balance between FarR and its ligand in order for proper activation of *farE*. Future experiments will be directed at determining the stoichiometry of FarR and its ligand.

Importantly, the $H_{121}Y$ substitution of FarR7 is located in the C-terminal ligand-binding domain of the protein, but it is the N-terminal domain that is involved in DNA recognition and binding. Given the location of the H121Y substitution, perhaps FarR7 adopts a conformation that mimics a ligand-bound state, leading to loss of affinity for O_{farR} and O_{PAL1}, but which also promotes the

ability to interact with O_{farE}. This could explain why de-repression of *farR* alone is insufficient to promote *farE* expression since the induction of *farE* expression would also be co-dependent on the presence of an activating ligand to promote interaction with the O_{farE} site.

The composition of promoter spacer DNA has been shown to influence promoter activity, such that AT-rich spacers are stronger promoters compared to those with GC-rich spacers (96, 97). The *farE* promoter contains a GC-rich spacer between the -10 and -35 promoter elements, indicating that a transcriptional activator is most likely needed. Additionally, the third operator site of FarR, O_{farE}, lies upstream of the *farE* promoter, the position of which is consistent with a role in activation. O_{farE} contains PAL2 which also contains a TAGWTTA motif. We have shown that a G>A point mutation in the TAGWTTA motif of O_{farE} caused a loss in resistance to linoleic acid (Fig 3.2A). Although we expected that this would cause a loss of affinity for O_{farE}, EMSA conducted with the full intergenic segment containing this G>A substitution did not reveal any obvious difference in the mobility shift pattern, including that the S3 shift which we had hypothesized to be due to interaction with O_{farE} and the TAGWTTA motif of PAL2 (Fig 3.2B). Conversely, EMSA done with a minimal PAL2 (OP4.1) probe revealed that FarR was unable to bind, even though FarR was able to bind to a minimal PAL1 probe (Fig 3.3B). However, it must be noted that all EMSA were performed in the absence of an exogenous ligand. As such, our data are consistent with the expectation that FarR must bind a fatty acid ligand in order to recognize the minimal PAL2 probe. FabR, a TFR in *E. coli* that represses genes for unsaturated fatty acid biosynthesis functions through a similar mechanism. FabR is only able to bind the canonical FabR binding site if it is extended by additional nucleotides. However, upon the addition of its cognate ligand, oleoyl-CoA or palmitoyl-CoA, it is then able to bind to a minimal motif (105).

The ability of FarR to both repress and activate expression *farE* is unusual, and therefore, FarR must be able to differentiate between repressing and activating operator sites. However, the three operator sites all contain the same TAGWTTA motif. Therefore, we speculate that the three TAGWTTA motifs within the intergenic segment of FarR all appear within a different context, allowing FarR to differentiate between them. The TAGWTTA motif of both O_{PAL1} and O_{farE} appears within PAL1 and PAL2, respectively, which are comprised of identical or near-identical inverted repeat half-sites. However, they differ in the positions of IR1 and IR2a, the orientation of

which are juxtaposed in PAL2 (Fig 3.3A). In *Streptococcus pneumoniae*, the TFR SczA is both an activator and repressor of the Zn^{2+} efflux pump CzcD. Similar to FarR, SczA recognizes a common TGTTCA motif in both a repressing and activating context. In the absence of Zn^{2+}, SczA binds to a TGTTCA motif within a perfect inverted repeat in which to repress *czcD* expression. In the presence of Zn^{2+}, SczA binds to an identical motif located within an imperfect repeat upstream (106). Perhaps through the binding of a ligand, FarR is able to differentiate between the juxtaposed inverted repeats of PAL1 and PAL2 in a similar fashion to SczA.

Another observation made from this study is when FarR is de-repressed and produced constitutively, there tends to be a decrease in resistance to uFFA (Fig 3.1D). Because of these observations, we speculate that FarR or FarE may be toxic to the cell in high amounts, explaining why FarR is so tightly regulated through auto-repression. This is similar in the case of tetracycline resistance. In *E. coli*, TetR belongs to the TFR and regulates the expression of *tetA*, a tetracycline efflux pump, and studies have shown that overproduction of TetA strongly reduces fitness (107). Another point to consider is whether FarE can discriminate between uFFA and other fatty acids synthesized by *S. aureus*, such as branched-chain fatty acids (BCFA), as RND family efflux pumps usually have a wide range of substrates (85, 86). *farE* and *farR* might be tightly regulated in order to ensure that FarE is only activated after an accumulation of uFFA metabolites and is turned off quickly once levels fall below the activating threshold, to prevent efflux of synthesized BCFA, which are important in maintaining membrane fluidity and are energetically expensive to synthesize (62).

This study has confirmed that the 5´UTR of the *farR* mRNA in itself is not sufficient to promote resistance to linoleic acid (Fig 3.4B). However, these findings do not exclude the possibility of regulation through small RNAs or riboswitches. Small RNAs (sRNA) are often utilized by both prokaryotes and eukaryotes. In prokaryotes, they are implicated in regulating a variety of genes, including those for plasmid maintenance through regulation of plasmid copy number or through toxin-antitoxin systems (110). Antisense sRNAs function to control gene regulation by base pairing to the 5´UTR of the target mRNA and inhibiting translation by blocking the RBS or destabilizing the mRNA. There are some examples of TFRs using sRNA as a post-transcriptional regulatory mechanism. In *M. smegmatis* AmtR is a global regulator of nitrogen metabolism. When

nitrogen is abundant, cis-encoded small RNAs (sRNA) complementary to *amtR* mRNA block transcription (95). Additionally, in *V. harveyi*, LuxR is an unusual member of the TetR family that functions as a global regulator to repress or activate target gene expression, and LuxR expression is regulated at the post-transcriptional level through sRNA molecules that destabilize the *luxR* mRNA transcript (76, 86). Regulation by sRNA would be beneficial in situations where protein synthesis bursts would be detrimental to fitness (110). Our observation that increased production of FarR tends to decrease resistance to uFFA supports this notion. Additionally, the 5´ ends of *farE* and *farR* mRNA overlap through 21nt that could negatively impact the stability or translation and could promote degradation through RNAse III, a dsRNA dependent ribonuclease in *S. aureus* (112). The 5´UTRs of the mRNA can also be involved in post-transcriptional regulation as metabolite binding-riboswitches. Metabolite-binding riboswitches alter gene expression at the post-transcriptional level through allosteric rearrangement in nearby mRNA structures (113). *farR* or *farE* mRNA may be able to bind fatty acid metabolites, which can allow for subsequent translation.

FarR contains two cysteine residues that we have shown to be important for function. Cysteine residues have shown to be important for the function of other regulators, both through redox reaction and through the participation in disulfide bonds. SarA in *S. aureus* regulates many genes including thioredoxin reductase *trxB*, and along with thioredoxin *trxA,* is important in maintaining a local thiol-disulfide balance within the cell. A study done by Ballal *et al.* found that Cys9 of SarA is important in the regulation of *trxB* (97). In non-oxidizing conditions, wildtype SarA binds to the *trxB* promoter to repress gene expression. It was shown through EMSA that when SarA is incubated with oxidizing agents such as H_2O_2 or diamine, there is a partial disruption of the SarA-*trxB* promoter complex. However, when EMSA was done with mutant SarA Cys9>Gly in the presence of oxidizing agents, there was no disruption of the SarA Cys9>Gly-promoter complex, indicating that the oxidation of Cys9 is important for SarA function (97). Additionally, cysteine residues have been shown to play a role in the oligomerization of TFRs. TFRs typically function as dimers; however, there are some TFRs that bind to DNA as a dimer of dimers. CprB is a TFR in *Streptomyces coelicolor* that regulates pigment production. CprB functions as a dimer of dimers, and it has been shown that disulfide bonds between dimer pairs through Cys159 of CprB is important for structural stability of the protein (114). Our data show that both cysteine residues of

FarR are important for function; however, it is unknown if their importance is for the sensing of oxidative/reductive environments, structural stability through disulfide bonds, or through another unknown mechanism (Fig 3.5B). The strongest known inducer of *farE* expression is arachidonic acid (56). Therefore, FarR being able to sense the oxidative environment of the cell may be beneficial as arachidonic acid has been shown to kill *S. aureus* through a lipid peroxidation mechanism, which creates an oxidative environment in the cell (48). C37 of FarR lies within the N-terminal DNA binding domain, and therefore, may be in part responsible for DNA binding. Additionally, when C37 is substituted for alanine, there is a complete lack of FarR detected in lysates, indicating that this C37A substitution may be influencing DNA binding through super-repression of FarR (Fig 3.5C). C116 lies within the C-terminal ligand-binding domain, and we have shown that variation of the amino acid sequence at this position can influence the relative abundance of FarR protein as evident through Western blot analysis of cell lysate. ^{C116Y}FarR was more readily detected than ^{C116A}FarR and slightly more than wildtype FarR. However, ^{C116Y}FarR was not detected to the same extent as ^{H121Y}FarR (Fig 3.6). As C116 lies in close proximity to H121, both are situated within the same α-helix, and both variants of FarR appear to be de-repressed compared to wild type, we speculated that a C116Y substitution may confer resistance to linoleic acid, as does FarR7 (H121Y). Additionally, a study done by Nguyen *et al.* has shown that a C116R substitution in FarR leads to constitutive expression of *farE* (98). Both tyrosine and arginine are larger amino acids than histidine and cysteine, and therefore may be able to extend into the ligand-binding pocket. This may cause FarR to adopt a ligand-bound conformation, explaining the de-repression of *farE* seen in the case of FarR H121Y and FarR C116R, and the de-repression of FarR we see in the case of H121Y and C116Y.

A defining characteristic of TFRs is their ability to bind a physiological ligand. However, this study was unable to confirm the identity of this ligand. TFRs usually bind to hydrophobic ligands, and previous studies in our lab indicate that in a USA300Δ*fakA* background, *farE* expression is constitutively elevated but cannot be induced (82). The USA300Δ*fakA* background exhibits a phenotype of an accumulation of non-esterified fatty acid metabolites, which may explain the increased basal level of *farE* expression (85). From these observations, we hypothesize that the ligand may be acyl-phosphates. We set out to co-express FakA, FakB2, FarR, and FarE in *E. coli*, as this approach in a heterologous host, if successful, would demonstrate the minimal genes

necessary to activate *farE* expression. Through Western blots, we determined that the presence of FakA, FakB2 and phosphorylated linoleic acid did not relieve autorepression of FarR upon the addition of linoleic acid. *E. coli* transformed with both pBAD*fakAB2* and pLI*farER* was grown to mid-exponential phase, at which point arabinose was added to induce the expression of FakA and FakB2, and 50 μM linoleic acid was added. Growth of *E. coli* DH5α was previously determined not to be affected by the presence of 50 μM linoleic acid, and therefore this concentration was chosen for the duration of this experiment. *E. coli* is able to incorporate exogenous fatty acid into phospholipid through acyl-CoA synthetase (FadD) (52, 92). Therefore, for future experiments, the subinhibitory concentration of linoleic acid will be determined to ensure that there is a buildup of acyl-phosphates within the cytosol.

We were unable to determine if the presence of FakA, FakB2, and phosphorylated linoleic acid induced *farE* expression as Western blots performed with anti-FarE-PD antibodies were unsuccessful. Anti-FarE-PD antibodies were able to detect FarE-PD but were unable to detect full FarE protein from either *E. coli* transformed with *farE* on an inducible promoter, or in USA300 grown in the presence of linoleic acid. The lack of detectable FarE from USA300 could be explained by the low abundance of FarE, even in inducing conditions. RND family efflux pumps efflux a wide range of substrates that are structurally related to their main target (109). FarE may be indiscriminately effluxing other fatty acids or membrane phospholipid derivatives, which would be detrimental to the cell, therefore, requiring tight regulation and only be expressed when needed. Additionally, the *farE* mRNA may in intrinsically unstable, again to limit the indiscriminate efflux of phospholipid derivatives, explaining the lack of detectable FarE-PD from *E. coli* lysates transformed with *farE* on an inducible plasmid.

Although our first line of investigation was to try to confirm acyl-phosphate as a physiological ligand for FarR, another possibility for the activation of *farE* expression is that FarR requires a co-activator protein, which may include FakA or FakB1/2. In *Lactococcus lactis,* dihydroxyacetone metabolism is regulated in a mechanism consisting of co-activator proteins. DhaQ binds the physiological ligand dihydroxyacetone. The DhaQ-dihydroxyacetone complex then binds to DhaS, a member of the TetR family. Only when DhaS binds the DhaQ-dihydroxyacetone complex can it activate genes for dihydroxyacetone metabolism (74). DhaS is also an unconventional TFR

in the respect that it is a transcriptional activator and not a repressor, similar to FarR. Additionally, FarR may also be able to sense changes in membrane composition due to the incorporation of linoleic acid similar to *esxA* activation. EsxA is a virulence factor in *S. aureus* that is secreted in response to linoleic acid in a mechanism dependent on the incorporation of linoleic acid into biosynthetic pathways by FakA. A decrease in the membrane fluidity due to the incorporation of linoleic acid is suggested as a signal that activates *esxA* expression (117).

Overall, our data support the following mechanism of action (Fig 4.1). In the absence of a ligand, FarR is bound to O_{farR} and O_{PAL1}, repressing transcription of both *farR* and *farE.* When exogenous unsaturated fatty acids enter the cell, they are bound by FakB2 and are then phosphorylated by FakA. The resulting acyl-phosphate is then incorporated into membrane phospholipid by the Pls acyltransferase system. Eventually, the buildup of acyl-phosphates exceeds the rate of incorporation by Pls, leading to a pool of acyl-phosphates within the cytosol. At this point, FarR binds either to the acyl-phosphates alone or to acyl-phosphates in a complex with FakA/B2, leading to loss of affinity for O_{farR}/O_{PAL1} and binding to O_{farE}, activating *farE* expression.

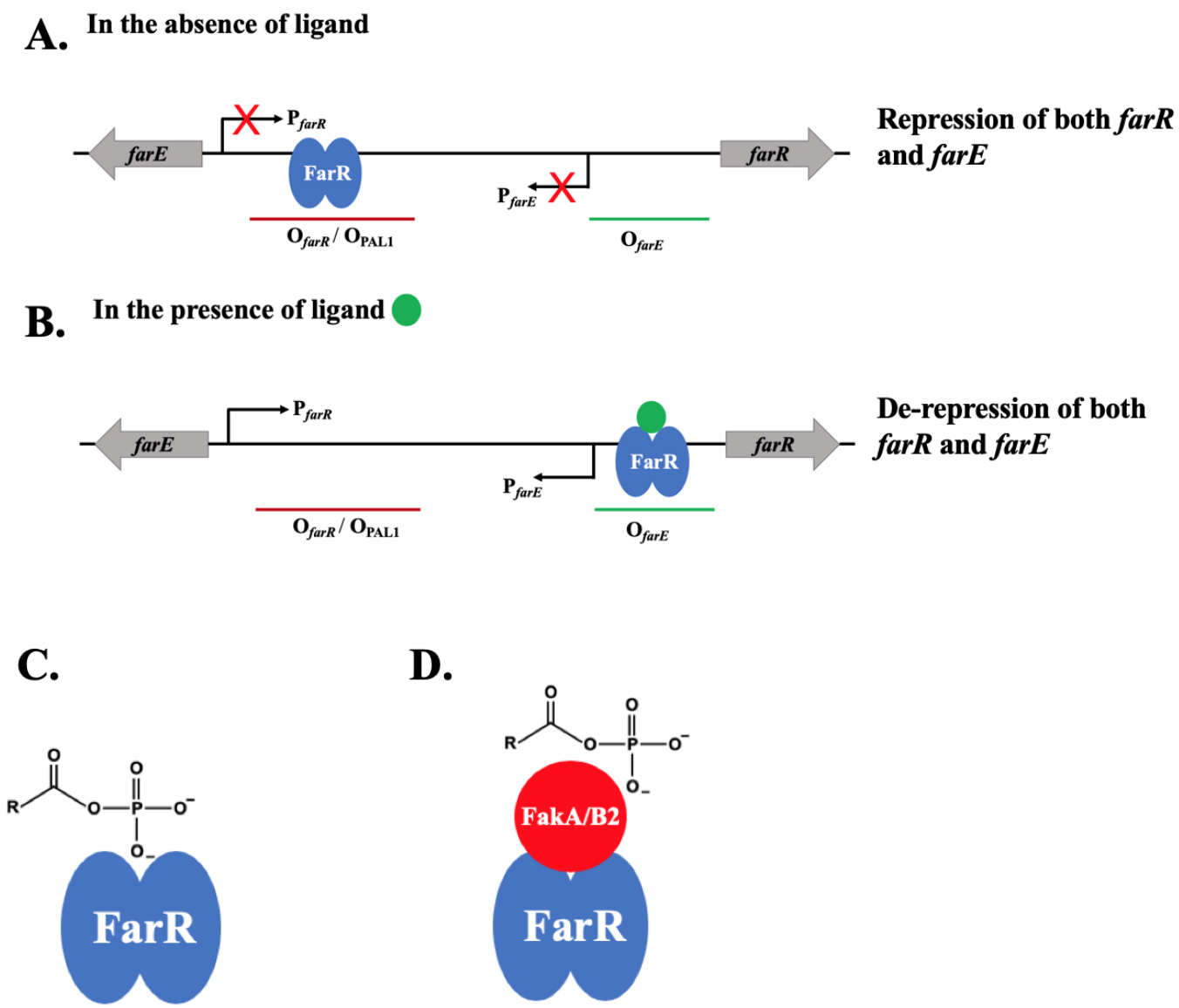

Figure 4.1 Proposed model for FarR function. (A) In the absence of ligand, FarR remains bound to the repressing operator site, O_{farR} and O_{PAL1}, inhibiting transcription of both *farR* and *farE*. **(B)** When bound to its ligand, FarR is able to bind to the proposed activating operator site O_{farE} to activate farE expression. Proposed ligands of FarR include **(C)** acyl-phosphates or **(D)** acyl-phosphates as a complex with FakA/B2.

This study was unable to determine the ligand of FarR and future research will be directed at elucidating the identity of this ligand. We hypothesize that the ligand may be acyl-phosphates on its own, or perhaps FakA/FakB2 acyl-phosphate complex. To determine if this is the case, FakA and FakB2 will be purified and an *in vitro* phosphorylation assay will be done to produce acyl-phosphates. The resulting cocktail will then be added to EMSA buffer to determine if the presence of FakA, FakB2, or phosphorylated linoleic acid modulated the DNA binding affinity of FarR for operator sites. For this purpose, we would use the minimal PAL2 probe, as this represents the site that is predicted to function in the activation of *farE* expression, and FarR fails to bind to minimal PAL2 in the absence of ligand. Additionally, if FarR behaves in a similar manner to DhaS, it may be binding to FakA/FakB2 in complex with an acyl-phosphate. To determine whether it is the acyl-phosphates alone, or a FakA/FakB2/acyl-phosphate complex, the acyl-phosphates will be separated via chloroform extraction prior to being used in EMSA. Future research will also be targeted at further understanding the role that cysteines play in FarR function. As we have determined that both Cys37 and Cys116 are important for the growth of USA300 at 50 μM linoleic acid. EMSA will be done with ^{C37A}FarR and ^{C116A}FarR to determine whether the cysteine residues are necessary for DNA binding.

In summary, we have studied the regulation of uFFA efflux pump FarE by TetR family transcriptional regulator FarR. Results of this study have provided evidence that FarR recognizes a conserved TAGWTTA that appears three times within the intergenic segment. We have shown that FarR is able to auto-repress its own expression through the cooperative binding of O_{PAL1} and O_{farR}; however, this de-repression of *farR* does not increase resistance to linoleic acid. This study has also identified the importance of cysteine residues in FarR function. The ligand of FarR is still yet to be determined. Cumulatively, these findings further elucidate the regulation of *farE*, and give us a better understanding of the mechanisms utilized by *S. aureus* to persist on and to colonize the human skin.

5 References

1. Brugger SD, Bomar L, Lemon KP. Commensal-pathogen interactions along the human nasal passages. PLoS Pathog. 2016;12(7):e1005633.
2. Williams R. Healthy carriage of *Staphylococcus aureus* : its prevalence and importance. Bacteriol Rev. 1963;27:56–67.
3. Wertheim HFL, Melles DC, Vos MC, Van Leeuwen W, Van Belkum A, Verbrugh HA, et al. The role of nasal carriage in *Staphylococcus aureus* infections. Lancet Infect Dis. 2005;5(12):751–62.
4. Kluytmans JAJW, Wertheim HFL. Nasal carriage of *Staphylococcus aureus* and prevention of nosocomial infections. Infection. 2005;33:3–8.
5. Kluytmans J, Van Belkum A, Verbrugh H. Nasal carriage of *Staphylococcus aureus*: epidemiology, underlying mechanisms, and associated risks. 1997;10(3):505–20.
6. Nouwen JL, Ott A, Kluytmans-Vandenbergh MFQ, Boelens H a M, Hofman A, van Belkum A, et al. Predicting the *Staphylococcus aureus* nasal carrier state: derivation and validation of a "culture rule". Clin Infect Dis. 2004;39(6):806–11.
7. Nouwen JL, Fieren MWJA, Snijders S, Verbrugh HA, Van Belkum A. Persistent (not intermittent) nasal carriage of *Staphylococcus aureus* is the determinant of CPD-related infections. Kidney Int. 2005;67:1084–92.
8. von Eiff C, Becker K, Machka K, Stammer H, Peters G. Nasal Carriage as a Source of *Staphylococcus aureus* bacteremia. N Engl J Med. 2001;344(1):11–6.
9. Sakr A, Brégeon F, Mège J-L, Rolain J-M. Staphylococcus aureus nasal colonization: an update on mechanisms, epidemiology, risk factors, and subsequent infections. Front Microbiol. 2018;9(2419).
10. Vazquez V, Liang X, Horndahl JK, Ganesh VK, Smeds E, Foster TJ, et al. Fibrinogen is a ligand for the *Staphylococcus aureus* microbial surface components recognizing adhesive matrix molecules (MSCRAMM) bone sialoprotein-binding protein (Bbp). J Biol Chem. 2011;286(34):29797–805.
11. Hammer ND, Skaar EP. Molecular mechanisms of *Staphylococcus aureus* iron acquisition. Annu Rev Microb. 2011;64:129–47.
12. Courcol RJ, Trivier D, Bissinger M-C, Martin GR, Brown MRW. Siderophore production

by *Staphylococcus aureus* and identification of iron-regulated proteins. Infect Immun. 1997;65(5):1944–8.

13. De Haas CJC, Veldkamp KE, Peschel A, Weerkamp F, Van Wamel WJB, Heezius ECJM, et al. Chemotaxis inhibitory protein of *Staphylococcus aureus* , a bacterial antiinflammatory agent. J Exp Med. 2004;199(5):687–95.
14. van Strijp G, M van Kessel Cristina Prat KP, Bestebroer J, C de Haas CJ. A new Staphylococcal anti-inflammatory protein that antagonizes the formyl peptide receptor like-1. J Immunol. 2006;177(11):8017–26.
15. Forsgren A, Nordström K. Protein A from *Staphylococcus aureus* : the biological significance of its reaction with IgG. Ann N Y Acad Sci. 1974 Jul;236(1):252–66.
16. Cosgrove K, Coutts G, Jonsson I-M, Tarkowski A, Kokai-Kun JF, Mond JJ, et al. Catalase (KatA) and Alkyl Hydroperoxide Reductase (AhpC) have compensatory roles in peroxide stress resistance and are required for survival, persistence, and nasal colonization in *Staphylococcus aureus*. J Bacteriol. 2007;189(3):1025–35.
17. Clauditz A, Resch A, Wieland K-P, Peschel A, Götz F. Staphyloxanthin plays a role in the fitness of *Staphylococcus aureus* and its ability to cope with oxidative stress. Infect Immun. 2006;74(8):4950–3.
18. Alonzo F, Benson MA, Chen J, Novick RP, Shopsin B, Torres VJ. *Staphylococcus aureus* leukocidin ED contributes to systemic infection by targeting neutrophils and promoting bacterial growth in vivo. Mol Microbiol. 2012;83(2):423–35.
19. Song L, Hobaugh MR, Shustak C, Cheley S, Bayley H, Eric Gouaux J. Structure of Staphylococcal α-hemolysin, a hepatameric transmembrane pore. Vol. 274, Science. 1996.
20. Kobayashi SD, Malachowa N, Deleo FR. Pathogenesis of *Staphylococcus aureus* Abscesses. Am J Pathol. 2015;185:1518–27.
21. Schwan WR, Langhorne MH, Ritchie HD, Stover CK. Loss of hemolysin expression in *Staphylococcus aureus agr* mutants correlates with selective survival during mixed infections in murine abscesses and wounds. FEMS Immunol Med Microbiol. 2003;38(1):23–8.
22. Berube BJ, Wardenburg JB. *Staphylococcus aureus* α-toxin: nearly a century of intrigue. Toxins (Basel). 2013 Jun 13;5:1140–66.
23. Jusko M, Potempa J, Kantyka T, Bielecka E, Miller HK, Kalinska M, et al.

Staphylococcal proteases aid in evasion of the human complement system. J Innate Immun. 2014;6:31–46.

24. Potempa J, Dubin A, Korzus G, Travis J. Degradation of elastin by a cysteine proteinase from *Staphylococcus aureus*. J Biol Chem. 1988;263(6):2664–7.
25. Arsic B, Zhu Y, Heinrichs DE, Mcgavin MJ. Induction of the Staphylococcal Proteolytic Cascade by Antimicrobial Fatty Acids in Community Acquired Methicillin Resistant *Staphylococcus aureus*.
26. McCormick JK, Yarwood JM, Schlievert PM. Toxic shock syndrome and bacterical superantigens: an update. Annu Rev Microbiol. 2001;55:77–104.
27. Donlan RM, William Costerton J. Biofilms: survival mechanisms of clinically relevant microorganisms. Clin Microbiol Rev. 2002;15(2):167–93.
28. Van Hal SJ, Jensen SO, Vaska VL, Espedido BA, Paterson DL, Gosbell IB. Predictors of mortality in *Staphylococcus aureus* bacteremia. Clin Microbiol Rev. 2012;25(2):362–86.
29. Chambers HF, DeLeo FR. Waves of resistance: Staphylococcus aureus in the antibiotic era. Nat Rev Microbiol. 2009;7(9):629–41.
30. Wei SW, Lencastre H DE, Tomasz A. Recruitment of the mecA gene homologue of Staphylococcus sciuri into a resistance determinant and expression of the resistant phenotype in *Staphylococcus aureus*. J Bacteriol. 2001;183(8):2417–24.
31. Valsesia G, Rossi M, Bertschy S, Pfyffer GE. Emergence of SCC*mec* type IV and SCC*mec* type V methicillin-resistant *Staphylococcus aureus* containing the Panton-Valentine Leukocidin genes in a large academic teaching hospital in central Switzerland: external invaders or persisting c. J Clin Microbiol. 2010;48(3):720–7.
32. Lee SM, Ender M, Adhikari R, Smith JMB, Berger-Bächi B, Cook GM. Fitness cost of Staphylococcal cassette chromosome *mec* in methicillin-resistant *Staphylococcus aureus* by way of continuous culture. Antimicrob Agents Chemother. 2007;51(4):1497–9.
33. Mediavilla JR, Chen L, Mathema B, Kreiswirth BN. Global epidemiology of community-associated methicillin resistant *Staphylococcus aureus* (CA-MRSA). Curr Opin Microbiol. 2012 Oct 1;15(5):588–95.
34. Enström J, Fröding I, Giske CG, Ininbergs K, Bai X, Sandh G, et al. USA300 methicillin-resistant *Staphylococcus aureus* in Stockholm, Sweden, from 2008 to 2016. PLoS One. 2018;13(11):e0205761.

35. McDougal LK, Steward CD, Killgore GE, Chaitram JM, Mcallister SK, Tenover FC. Pulsed-field gel electrophoresis typing of oxacillin-resistant *Staphylococcus aureus* isolates from the United States: establishing a national database. J Clin Microbiol. 2003;41(11):5113–20.
36. Enright MC, Robinson DA, Randle G, Feil EJ, Grundmann H, Spratt BG. The evolutionary history of methicillin-resistant *Staphylococcus aureus* (MRSA). PNAS. 2002;99(11):7687–92.
37. Thurlow LR, Joshi GS, Richardson AR. Virulence strategies of the dominant USA300 lineage of community associated methicillin resistant *Staphylococcus aureus* (CA-MRSA). FEMS Immunol Med Microbiol. 2012;65(1):5–22.
38. Glaser P, Martins-Simões P, Villain A, Barbier M, Tristan A, Bouchier C, et al. Demography and intercontinental spread of the USA300 community-acquired methicillin-resistant *Staphylococcus aureus* lineage. MBio. 2016;7(1):e02183-15.
39. Laupland KB, Ross T, Gregson DB. *Staphylococcus aureus* bloodstream infections: risk factors, outcomes, and the influence of methicillin resistance in Calgary, Canada, 2000-2006. J Infect Dis. 2008;198(3):336–43.
40. Christianson S, Golding GR, Campbell J, Mulvey MR. Comparative genomics of Canadian epidemic lineages of methicillin-resistant *Staphylococcus aureus*. J Clin Microbiol. 2007;45(6):1904–11.
41. Proksch E, Brandner JM, Jensen J-M. The skin: an indispensable barrier. Exp Dermatol. 2008;17:1063–72.
42. Elias PM. The skin barrier as an innate immune element. Semin Immunopathol. 2007;29:3–14.
43. Drake DR, Brogden KA, Dawson D V, Wertz PW. Antimicrobial lipids at the skin surface. J Lipid Res. 2008;49(1):4–11.
44. Do TQ, Moshkani S, Castillo P, Anunta S, Pogosyan A, Cheung A, et al. Lipids Including cholesteryl linoleate and cholesteryl arachidonate contribute to the inherent antibacterial activity of human nasal fluid. J Immunol. 2008;181(6):4177–87.
45. Shryock TR, Kapral FA. The production of bactericidal fatty acids from glycerides in staphylococcal abscesses. J Med Microbiol. 1992;36(42):288–92.
46. Parsons JB, Yao J, Frank MW, Jackson P, Rock CO. Membrane disruption by

antimicrobial fatty acids releases low-molecular-weight proteins from *Staphylococcus aureus*. J Bacteriol. 2012;194(19):5294–304.

47. Takigawa H, Nakagawa H, Kuzukawa M, Mori H, Imokawa G. Deficient production of hexadecenoic acid in the skin Is associated in part with the vulnerability of atopic dermatitis patients to colonization by *Staphylococcus aureus*. Dermatology. 2005;211:240–8.
48. Beavers WN, Monteith AJ, Amarnath V, Mernaugh RL, Roberts LJ, Chazin WJ, et al. Arachidonic acid kills *Staphylococcus aureus* through a lipid peroxidation mechanism. MBio. 2019;10(5):e01333-19.
49. Planet PJ, LaRussa SJ, Dana A, Smith H, Xu A, Ryan C, et al. Emergence of the epidemic methicillin-resistant *Staphylococcus aureus* strain USA300 coincides with horizontal transfer of the arginine catabolic mobile element and *speG*-mediated adaptations for survival on skin. MBio. 2013;4(6):e00889-13.
50. Thurlow LR, Joshi GS, Clark R, Spontak JS, Neely CJ, Maile R, et al. Functional modularity of the arginine catabolic mobile element contributes to the success of USA300 methicillin-resistant *Staphylococcus aureus*. Cell Host Microbe. 2013;13(1):100–7.
51. Chamberlain NR, Mehrtens BG, Xiong Z, Kapral FA, Boardman JL, Rearick4 JI. Correlation of carotenoid production, decreased membrane fluidity, and resistance to oleic acid killing in *Staphylococcus aureus* 18Z. Infect Immun. 1991;59(12):4332–7.
52. Kenny JG, Ward D, Josefsson E, Jonsson I-M, Hinds J, Rees HH, et al. The *Staphylococcus aureus* response to unsaturated long chain free fatty acids: survival mechanisms and virulence implications. Davis D, editor. PLoS One. 2009;4(2):e4344.
53. Clarke SR, Mohamed R, Bian L, Routh AF, Kokai-Kun JF, Mond JJ, et al. The *Staphylococcus aureus* surface protein IsdA mediates resistance to innate defenses of human skin. Cell Host Microbe. 2007;1:199–212.
54. Kohler T, Weidenmaier C, Peschel A. Wall teichoic acid protects *Staphylococcus aureus* against antimicrobial fatty acids from human skin. J Bacteriol. 2009;191(13):4482–4.
55. Truong-Bolduc QC, Bolduc GR, Medeiros H, Vyas JM, Wang Y, Hooper DC. Role of the Tet38 efflux pump in *Staphylococcus aureus* internalization and survival in epithelial cells. Infect Immun. 2015;83(11):4362–72.
56. Alnaseri H, Arsic B, Schneider JET, Kaiser JC, Scinocca ZC, Heinrichs DE, et al.

Inducible expression of a resistance-nodulation-division-type efflux pump in *Staphylococcus aureus* provides resistance to linoleic and arachidonic acids. J Bacteriol. 2015;197(11):1893–905.

57. Kapral FA, Smith S, Lal D. The esterification of fatty acids by *Staphylococcus aureus* fatty acid modifying enzyme (FAME) and its inhibition by glycerides. J Med Microbiol. 1992;37:235–7.
58. Parsons JB, Broussard TC, Bose JL, Rosch JW, Jackson P, Subramanian C, et al. Identification of a two-component fatty acid kinase responsible for host fatty acid incorporation by *Staphylococcus aureus*. PNAS. 2014;111(29):10532–7.
59. Kuhn S, Slavetinsky CJ, Peschel A. Synthesis and function of phospholipids in *Staphylococcus aureus*. Int J Med Microbiol. 2015;305(2):196–202.
60. Aguilar PS, Cronan JE, de Mendoza D. A *Bacillus subtilis* gene induced by cold shock encodes a membrane phospholipid desaturase. J Bacteriol. 1998;180(8):2194–200.
61. Kaneda T. Iso-and anteiso-fatty acids in bacteria: biosynthesis, function, and taxonomic significance. Microbiol Rev. 1991;55(2):288–302.
62. Singh VK, Hattangady DS, Giotis ES, Singh AK, Chamberlain NR, Stuart MK, et al. Insertional inactivation of branched-chain alpha-keto acid dehydrogenase in *Staphylococcus aureus* leads to decreased branched-chain membrane fatty acid content and increased susceptibility to certain stresses. Appl Environ Microbiol. 2008 Oct;74(19):5882–90.
63. Chaudhuri RR, Allen AG, Owen PJ, Shalom G, Stone K, Harrison M, et al. Comprehensive identification of essential *Staphylococcus aureus* genes using transposon-mediated differential hybridisation (TMDH). BMC Genomics. 2009;10:291.
64. Parsons JB, Frank MW, Jackson P, Subramanian C, Rock CO. Incorporation of extracellular fatty acids by a fatty acid kinase-dependent pathway in *Staphylococcus aureus*. Mol Microbiol. 2014;92(2):234–45.
65. Fernando DM, Kumar A. Resistance-nodulation-division multidrug efflux pumps in Gram-negative bacteria: role in virulence. Antibiotics. 2013;2(1):163–81.
66. Kim EH, Nies DH, McEvoy MM, Rensing C. Switch or funnel: how RND-type transport systems control periplasmic metal homeostasis. J Bacteriol. 2011;193(10):2381–7.
67. Chim N, Torres R, Liu Y, Capri J, Batot G, Whitelegge JP, et al. The structure and

interactions of periplasmic domains of crucial MmpL membrane proteins from *Mycobacterium tuberculosis*. Chem Biol. 2015;22(8):1098–107.

68. Halucha J. Investigating the functional relationships of RND efflux pumps in methicillin resistant *Staphylococcus aureus*. Electron Thesis Diss Repos. 2017;(4936).
69. Quiblier C, Zinkernagel AS, Schuepbach RA, Berger-Bächi B, Senn MM. Contribution of SecDF to *Staphylococcus aureus* resistance and expression of virulence factors. BMC Microbiol. 2011;11(72).
70. Cuthbertson L, Nodwell JR. The TetR family of regulators. Microbiol Mol Biol Rev. 2013;77(3):440–75.
71. Fromknecht K, Vogel PD, Wise JG. Combinatorial redesign of the DNA binding specificity of a prokaryotic helix-turn-helix repressor. J Bacteriol. 2003;185(2):475–81.
72. Pérez-Rueda E, Collado-Vides J. Common history at the origin of the position-function correlation in transcriptional regulators in archaea and bacteria. J Mol Evol. 2001;53:172–9.
73. Orth P, Cordes F, Schnappinger D, Hillen W, Saenger W, Hinrichs W. Conformational changes of the Tet repressor induced by tetracycline trapping. J Mol Biol. 1998;279(2):439–47.
74. Christen S, Srinivas A, Bähler P, Zeller A, Pridmore D, Bieniossek C, et al. Regulation of the Dha operon of *Lactococcus lactis*: a deviation from the rule followed by the TetR family of transcription regulators. J Biol Chem. 2006;281(32):23129–37.
75. Schumacher MA, Miller MC, Grkovic S, Brown MH, Skurray RA, Brennan RG. Structural basis for cooperative DNA binding by two dimers of the multidrug-binding protein QacR. EMBO J. 2002;21(5):1210–8.
76. Grkovic S, Brown MH, Roberts NJ, Paulsen IT, Skurray RA. QacR is a repressor protein that regulates expression of the *Staphylococcus aureus* multidrug efflux pump QacA. J Biol Chem. 1998;273(29):18665–73.
77. Grkovic S, Brown MH, Schumacher MA, Brennan RG, Skurray RA. The staphylococcal QacR multidrug regulator binds a correctly spaced operator as a pair of dimers. J Bacteriol. 2001;183(24):7102–9.
78. Yu D, Zhao L, Xue T, Sun B. Staphylococcus aureus autoinducer-2 quorum sensing decreases biofilm formation in an icaR-dependent manner. BMC Microbiol. 2012;12:288.

79. Jefferson KK, Cramton SE, Götz F, Pier GB. Identification of a 5-nucleotide sequence that controls expression of the ica locus in *Staphylococcus aureus* and characterization of the DNA-binding properties of IcaR. Mol Microbiol. 2003;48(4):889–99.
80. Truong-Bolduc QC, Villet RA, Estabrooks ZA, Hooper DC. Native efflux pumps contribute resistance to antimicrobials of skin and the ability of *Staphylococcus aureus* to colonize Skin. J Infect Dis. 2014;209:1485–93.
81. Alnaseri H. Identification and characterization of FarR and FarE as a regulator and effector of fatty acid resistance in *Staphylococcus aureus*. Electron Thesis Diss Repos. 2017;(5131).
82. Alnaseri H, Kuiack RC, Ferguson KA, Schneider JET, Heinrichs DE, McGavin MJ. DNA binding and sensor specificity of FarR; A novel TetR family regulator required for induction of the fatty acid efflux pump FarE in *Staphylococcus aureus*. J Bacteriol. 2019 Nov 19;201(3):e00602-18.
83. Fujihashi M, Nakatani T, Hirooka K, Matsuoka H, Fujita Y, Miki K. Structural characterization of a ligand-bound form of *Bacillus subtilis* FadR involved in the regulation of fatty acid degradation. Proteins. 2014;82(7):1301–10.
84. Agari Y, Agari K, Sakamoto K, Kuramitsu S, Shinkai A. TetR-family transcriptional repressor *Thermus thermophilus* FadR controls fatty acid degradation. Microbiology. 2011;157(6):1589–601.
85. Ericson ME, Subramanian C, Frank MW, Rock CO. Role of fatty acid kinase in cellular lipid homeostasis and SaeRS-dependent virulence factor expression in *Staphylococcus aureus*. MBio. 2017;8(4):e00988-17.
86. Novick RP. Genetic systems in Staphylococci. Methods Enzymol. 1991;204:587–636.
87. Feldgarden M, Cosimi L, Nicol R, Calderwood M, Huang S, Onderdonk A, et al. The genome sequences of *Staphylococcus aureus* M0049. The Broad Institute Genome Sequencing Platform, The Broad Institute Genome Sequncing Center for Infectious Disease.
88. Feldgarden M, Cosimi L, Nicol R, Calderwood M, Huang S, Onderdonk A, et al. The genome sequences of Staphylococcus aureus M0330. The Broad Institute Genome Sequencing Platform, The Broad Institute Genome Sequncing Center for Infectious Disease.

89. Feldgarden M, Cosimi L, Nicol R, Calderwood M, Huang S, Onderdonk A, et al. The genome sequences of *Staphylococcus aureus* M0390. The Broad Institute Genome Sequencing Platform, The Broad Institute Genome Sequncing Center for Infectious Disease.
90. Feldgarden M, Cosimi L, Nicol R, Calderwood M, Huang S, Onderdonk A, et al. The genome sequences of *Staphylococcus aureus* M0398. The Broad Institute Genome Sequencing Platform, The Broad Institute Genome Sequncing Center for Infectious Disease.
91. Feldgarden M, Cosimi L, Nicol R, Calderwood M, Huang S, Onderdonk A, et al. The genome sequences of *Staphylococcus aureus* M0423. The Broad Institute Genome Sequencing Platform, The Broad Institute Genome Sequncing Center for Infectious Disease.
92. Feldgarden M, Cosimi L, Nicol R, Calderwood M, Huang S, Onderdonk A, et al. The genome sequences of *Staphylococcus aureus* M1545. The Broad Institute Genome Sequencing Platform, The Broad Institute Genome Sequncing Center for Infectious Disease.
93. Lee CY, Iandolo JJ. Lysogenic conversion of staphylococcal lipase is caused by insertion of the bacteriophage L54a genome into the lipase structural gene. J Bacteriol. 1986 May;166(2):385–91.
94. Guzman L-M, Belin D, Carson MJ, Beckwith J. Tight regulation, modulation, and high-level expression by vectors containing the arabinose PBAD promoter. J Bacteriol. 1995;177(14):4121–30.
95. Petridis M, Vickers C, Robson J, Mckenzie JL, Bereza M, Sharrock A, et al. Structure and function of AmtR in *Mycobacterium smegmatis*: implications for post-transcriptional regulation of urea metabolism through a small antisense RNA. J Mol Biol. 2016;428(21):4315–29.
96. Tu KC, Waters CM, Svenningsen SL, Bassler BL. A small-RNA-mediated negative feedback loop controls quorum-sensing dynamics in Vibrio harveyi. Mol Microbiol. 2008;70(4):896–907.
97. Ballal A, Manna AC. Control of thioredoxin reductase gene (trxB) transcription by SarA in *Staphylococcus aureus*. J Bacteriol. 2010;192(1):336–45.

98. Nguyen M-T, Saising J, Tribelli PM, Nega M, Diene SM, François P, et al. Inactivation of *farR* causes high rhodomyrtone resistance and increased pathogenicity in *Staphylococcus aureus*. Front Microbiol. 2019;10(1157).
99. Magnuson K, Jackowski S, Rock CO, Cronan JE. Regulation of fatty acid biosynthesis in *Escherichia coli*. Microbiol Rev. 1993;57(3):522–42.
100. Fischer N, Kandt C. Porter domain opening and closing motions in the multi-drug efflux transporter AcrB. Biochim Biophys Acta Biomembr. 2013;1828:632–41.
101. Shryock TR, Dyef ES, Kapral FA. The accumulation of bactericidal lipids in staphylococcal abscesses. J Med Microbiol. 1992;36:332–6.
102. Liang JL, Nie Y, Wang M, Xiong G, Wang Y-P, Maser E, et al. Regulation of alkane degradation pathway by a TetR family repressor via an autoregulation positive feedback mechanism in a Gram-positive *Dietzia* bacterium. Mol Microbiol. 2016;99(2):338–59.
103. Hook-Barnard IG, Hinton DM. The promoter spacer influences transcription initiation via 70 region 1.1 of *Escherichia coli* RNA polymerase. PNAS. 2009;106(3):737–42.
104. Liu M, Tolstorukov M, Zhurkin V, Garges S, Adhya S. A mutant spacer sequence between -35 and -10 elements makes the Plac promoter hyperactive and cAMP receptor protein-independent. PNAS. 2004;101(18):6911–6.
105. Feng Y, Cronan JE. Complex binding of the FabR repressor of bacterial unsaturated fatty acid biosynthesis to its cognate promoters. Mol Microbiol. 2011;80(1):195–218.
106. Kloosterman TG, Van Der Kooi-Pol MM, Bijlsma JJE, Kuipers OP. The novel transcriptional regulator SczA mediates protection against Zn2+ stress by activation of the Zn2+-resistance gene *czcD* in *Streptococcus pneumoniae*. Mol Microbiol. 2007;65(4):1049–63.
107. Moyed HS, Nguyen TT, Bertrand KP. Multicopy Tn*1O tet* plasmids confer sensitivity to induction of *tet* gene expression. J Bacteriol. 1983;155(2):549–56.
108. Elkins CA, Nikaido H. Substrate specificity of the RND-type multidrug efflux pumps AcrB and AcrD of *Escherichia coli* is determined predominantly by two large periplasmic loops. J Bacteriol. 2002;184(23):6490–8.
109. Nikaido H. Structure and mechanism of RND-type multidrug efflux pumps. Adv Enzymol Relat Areas Mol Biol. 2010;77:1–60.
110. Levine E, Zhang Z, Kuhlman T, Hwa T. Quantitative characteristics of gene regulation by

small RNA. PLoS Biol. 2007;5(9):e229.

111. Pompeani AJ, Irgon JJ, Berger MF, Bulyk ML, Wingreen NS, Bassler BL. The *Vibrio harveyi* master quorum-sensing regulator, LuxR, a TetR-type protein is both an activator and a repressor: DNA recognition and binding specificity at target promoters. Mol Microbiol. 2008;70(1):76–88.
112. Lioliou E, Sharma CM, Caldelari I, Helfer A-C, Fechter P, Vandenesch F, et al. Global regulatory functions of the *Staphylococcus aureus* endoribonuclease III in gene expression. PLoS Genet. 2012;8(6):e1002782.
113. Barrick JE, Breaker RR. The distributions, mechanisms, and structures of metabolite-binding riboswitches. Genome Biol. 2007;8(11):R239.
114. Bhukya H, Bhujbalrao R, Bitra A, Anand R. Structural and functional basis of transcriptional regulation by TetR family protein CprB from *S. coelicolor* A3(2). Nucleic Acids Res. 2014;42(15).
115. Yao J, Rock CO. Exogenous fatty acid metabolism in bacteria. Biochimie. 2017;141:30–9.
116. Parsons JB, Rock CO. Bacterial lipids: metabolism and membrane homeostasis. Prog Lipid Res. 2013;52:249–76.
117. Lopez MS, Tan IS, Yan D, Kang J, McCreary M, Modrusan Z, et al. Host-derived fatty acids activate type VII secretion in *Staphylococcus aureus*. Proc Natl Acad Sci U S A. 2017;114(42):11223–8.

6 Curriculum Vitae

Name: Katherine A. Ferguson

Education:
MSc. In Microbiology and Immunology, 2020
Western University, London, Ontario, Canada

BMSc. Honours Specialization in Microbiology and Immunology, 2018
Western University, London, Ontario, Canada

Honours and Awards:
NSERC-Canadian Graduate Research Scholarship, 2019-2020

Western Graduate Research Scholarship, 2018-2020

Dr. FW Luney Graduate Entrance Scholarship, 2018

Western University Entrance Scholarship, 2014-2018

Dean's Undergraduate Research Opportunity, 2017

Related Work Experience:
Teaching Assistant, MicroImm 3100A, 2018-2019
Western University, London, Ontario, Canada

Committee Membership:
Infection and Immunity Research Forum Organizing Committee 2019

Publications:
Alnaseri, H., Kuiack, R.C., Ferguson, K.A., Schneider, J.E.T., Heinrichs D.E., McGavin, M.J. 2019. DNA binding and sensor specificity of FarR; a novel TetR family regulator required for induction of the fatty acid efflux pump FarE in *Staphylococcus aureus. J bacteriol.* 201:e00602-18.

Poster Presentations:

Regulation of Fatty Acid Efflux Pump FarE by TetR family transcriptional regulator FarR in *Staphylococcus aureus.* Infection and Immunity Research Forum. Poster Presentation. November 2019. London, ON, Canada

Regulation of Fatty Acid Efflux Pump FarE by TetR family transcriptional regulator FarR in *Staphylococcus aureus.* 69th Annual Conference of the Canadian Society of Microbiologists. Poster Presentation. June 2019. Sherbrooke, QC, Canada

Regulation of Fatty Acid Efflux Pump FarE by TetR family transcriptional regulator FarR in *Staphylococcus aureus.* London Health Research Day. Poster Presentation. May 2019. London, ON, Canada

Regulation of Fatty Acid Efflux Pump FarE by TetR family transcriptional regulator FarR in *Staphylococcus aureus.* Infection and Immunity Research Forum. Poster Presentation. October 2018. Stratford, ON, Canada

Regulation of Fatty Acid Efflux Pump FarE by TetR family transcriptional regulator FarR in *Staphylococcus aureus.* Infection and Immunity Research Forum. Poster Presentation. October 2017. London, ON, Canada